




RESEARCH ARTICLE

Integrative Cardiovascular Physiology and Pathophysiology

## Functional resilience of C57BL/6J mouse heart to dietary fat overload

Satya Murthy Tadinada,<sup>1,3</sup>  Eric T. Weatherford,<sup>2,3</sup>  Greg V. Collins,<sup>3</sup> Gourav Bhardwaj,<sup>3</sup> Jesse Cochran,<sup>3</sup> William Kutschke,<sup>4</sup> Kathy Zimmerman,<sup>4</sup> Alyssa Bosko,<sup>2</sup> Brian T. O'Neill,<sup>2,3,5</sup> Robert M. Weiss,<sup>4,6</sup> and  E. Dale Abel<sup>2,3</sup>

<sup>1</sup>Department of Neuroscience and Pharmacology, Carver College of Medicine, University of Iowa, Iowa City, Iowa; <sup>2</sup>Division of Endocrinology and Metabolism, Department of Internal Medicine, Carver College of Medicine, University of Iowa, Iowa City, Iowa; <sup>3</sup>Fraternal Order of Eagles Diabetes Research Center, Carver College of Medicine, University of Iowa, Iowa City, Iowa; <sup>4</sup>Abboud Cardiovascular Research Center, Carver College of Medicine, University of Iowa, Iowa City, Iowa; <sup>5</sup>Veterans Affairs Health Care System, Iowa City, Iowa; and <sup>6</sup>Division of Cardiology, Department of Internal Medicine, Carver College of Medicine, University of Iowa, Iowa City, Iowa

### Abstract

Molecular mechanisms underlying cardiac dysfunction and subsequent heart failure in diabetic cardiomyopathy are incompletely understood. Initially we intended to test the role of G protein-coupled receptor kinase 2 (GRK2), a potential mediator of cardiac dysfunction in diabetic cardiomyopathy, but found that control animals on HFD did not develop cardiomyopathy. Cardiac function was preserved in both wild-type and *GRK2* knockout animals fed high-fat diet as indicated by preserved left ventricular ejection fraction (LVEF) although heart mass was increased. The absence of cardiac dysfunction led us to rigorously evaluate the utility of diet-induced obesity to model diabetic cardiomyopathy in mice. Using pure C57BL/6J animals and various diets formulated with different sources of fat-lard (32% saturated fat, 68% unsaturated fat) or hydrogenated coconut oil (95% saturated fat), we consistently observed left ventricular hypertrophy, preserved LVEF, and preserved contractility measured by invasive hemodynamics in animals fed high-fat diet. Gene expression patterns that characterize pathological hypertrophy were not induced, but a modest induction of various collagen isoforms and matrix metalloproteinases was observed in heart with high-fat diet feeding. PPAR $\alpha$ -target genes that enhance lipid utilization such as *Pdk4*, *CD36*, *AcadL*, and *Cpt1b* were induced, but mitochondrial energetics was not impaired. These results suggest that although long-term fat feeding in mice induces cardiac hypertrophy and increases cardiac fatty acid metabolism, it may not be sufficient to activate pathological hypertrophic mechanisms that impair cardiac function or induce cardiac fibrosis. Thus, additional factors that are currently not understood may contribute to the cardiac abnormalities previously reported by many groups.

**NEW & NOTEWORTHY** Dietary fat overload (DFO) is widely used to model diabetic cardiomyopathy but the utility of this model is controversial. We comprehensively characterized cardiac contractile and mitochondrial function in C57BL/6J mice fed with lard-based or saturated fat-enriched diets initiated at two ages. Despite cardiac hypertrophy, contractile and mitochondrial function is preserved, and molecular adaptations likely limit lipotoxicity. The resilience of these hearts to DFO underscores the need to develop robust alternative models of diabetic cardiomyopathy.

*cardiac function; diabetic cardiomyopathy; high-fat diet; mitochondria; type 2 diabetes*

### INTRODUCTION

Cardiovascular disease (CVD) is the leading cause of death in the United States with an increasing incidence over the last three decades, driven in part by the increasing prevalence of obesity and diabetes (1). It is widely accepted that type 2 diabetes (2–4) and obesity (5, 6) increases the risk of heart failure.

G protein-coupled receptor kinase 2 (GRK2) is a Ser/Thr kinase that phosphorylates agonist activated GPCRs and

contributes to desensitization and downregulation of  $\beta$ -adrenergic receptors in the heart, among other GPCRs (7–9). A pathological role for GRK2 in various models of hypertrophy and heart failure has been previously reported (10–16). Cardiac GRK2 protein levels are elevated in the right atria of humans with diabetes mellitus and in the hearts of mice fed high-fat diet (17, 18). In the context of cardiac metabolism, GRK2 has been shown to decrease mitochondrial fatty acid oxidation and increase reactive oxygen species



generation in cardiomyocytes (19–21). However, whether GRK2 contributes to the development and/or progression of diabetic cardiomyopathy is not completely understood.

Various mouse models either genetic, or secondary to obesogenic diets have been used to model diabetic cardiomyopathy. Impaired contractile function has been reported in leptin receptor mutant models including *db/db* mice (22–24) and in leptin-deficient *ob/ob* mice (25, 26), which are characterized by hyperphagia, obesity, severe insulin resistance, and diabetes. Specifically, these animals develop cardiac hypertrophy and compromised systolic function, accompanied by changes in myocardial substrate utilization (22, 24, 27) reflected as reduced glucose oxidation, increased fatty acid oxidation, and myocardial lipid accumulation (22, 24, 27). An association between lipid accumulation and impaired cardiac function was also evident in transgenic overexpression models of genes involved in fatty acid oxidation such as acyl-CoA synthase (28). These studies suggest that lipotoxicity might be a key contributor to development of cardiac dysfunction when excess fatty acid uptake is not matched with increased fatty acid utilization. Other studies in models with increased triglyceride formation such as the cardiac overexpression of diacylglycerol transferase 1 (*DGAT1*), however, challenge the notion that triglyceride accumulation per se is sufficient to cause lipotoxic cardiomyopathy (29). Whether or not these models reflect the cardiac dysfunction associated with diabetes and obesity is unclear given that many of these transgenes and mutants are expressed throughout development.

Given that mice can develop many of the metabolic perturbations characteristic of poorly controlled type 2 diabetes with caloric excess in susceptible rodent strains, many investigators have used high-fat diet feeding up to 25 wk in rodents to model cardiac dysfunction in dysmetabolic states in the absence of genetic manipulations (30, 31). However, the reproducibility and reliability of the long-term fat feeding model for studying cardiac dysfunction associated with diabetes and obesity have been debated (32, 33) and warrant further investigation into additional factors such as environmental, background strain, and source of dietary fat. The goal of the current study was to initially investigate whether knockout of GRK2 in cardiomyocytes preserved cardiac function following long-term high-fat feeding in mice. In contrast with a few reports (30, 31) and in line with others (32, 33), our results revealed that wild-type animals with intact GRK2 expression in cardiomyocytes failed to develop cardiac dysfunction rendering us unable to conclusively define the precise role of GRK2 in diabetic cardiomyopathy. Given widespread use of the long-term high-fat diet feeding model, we sought to rigorously evaluate the structural, functional, mitochondrial, and transcriptional adaptations in the hearts of C57BL6/J to high-fat feeding as a function of age at diet initiation and fatty acid saturation of the dietary fat. Our findings caution using this preclinical model for identifying disease mechanisms and for developing targeted therapies for diabetic cardiomyopathy.

## METHODS

### Animals and Diets

All the protocols for animal use were approved by the Institutional Animal Care and Use Committee (IACUC) at the

University of Iowa. GRK2 floxed animals (exon 4) were provided by Dr. Yang K. Xiang (UC Davis) and were maintained on a mixed background. Cardiomyocyte specific inducible GRK2 knockout animals were generated by crossing GRK2<sup>fl/fl</sup> animals on a mixed background (C57BL6 and SV129) with Myh6-Cre<sup>ERT2</sup> mice (Stock No. 005657, Jackson Laboratories, Bar Harbor, ME). GRK2 knockout was induced by injections with tamoxifen (10 mg/kg/day) for 5 days at the age of 6 wk. Studies evaluating the effects of age at the time of initiation of HFD and fatty acid saturation on cardiac function were performed in C57BL/6J animals (Stock No. 000664, Jackson Laboratories, Bar Harbor, ME). Mice were purchased at 8 wk of age or 18 wk of age and were acclimatized in the animal facility at the University of Iowa for 1–2 wk. Only male mice were used in all the studies using C57BL6/J animals, as metabolic perturbations induced by high-fat feeding were comparable in male and female mice in the GRK2 high-fat diet study (data not shown). Animals were maintained on 12-h:12-h light/dark cycle with access to food and water ad lib. All animals were euthanized in the random-fed state at the end of the study. Formulated diets (Cat. Nos. D12450J, D12492 and custom ordered: low-fat low-sucrose (LFLS), low-fat high-sucrose (LFHS), and high-fat high-sucrose (HFHS)) were purchased from Research Diets (New Brunswick, NJ). The caloric contributions and fatty acid composition of custom-ordered diets are provided in Supplemental Table S1 (see <https://doi.org/10.6084/m9.figshare.15050718>).

### Western Blot Analysis

Knockout of GRK2 was validated by immunoblot (Supplemental Fig. S1; see <https://doi.org/10.6084/m9.figshare.15050733>) using GRK2 antibody (sc13143, Santa Cruz Biotechnology, Dallas, TX) and using  $\alpha$ -tubulin (cs 2144S, Cell Signaling, Danvers, MA) as loading control as described previously (34). Briefly, whole heart lysates were separated on 4%–12% NuPAGE gels (Invitrogen, Waltham, MA) using MES running buffer (Invitrogen, Waltham, MA) followed by transfer of separated proteins on to PVDF membranes (Immobilon-P, Sigma-Aldrich, St. Louis, MO). Overnight incubation with primary antibodies (used at 1:1,000 dilution) was performed after blocking the membranes with 5% BSA solution at room temperature for 1 h. Detection of target proteins was performed on a LI-COR Odyssey CLx scanner (LI-COR, Lincoln, NE) after 1-h incubation of membranes at room temperature with secondary antibodies (used at 1:10,000 dilution) tagged with fluorophores excitable at 700 nm or 800 nm (Cell Signaling, Danvers, MA). Image studio Lite was used for densitometric analysis. A ratio of GRK2 to respective  $\alpha$ -tubulin band intensities was used to adjust for differences in sample loading. Data were normalized to the mean value of control group and presented as relative change to the control group, which was set as 1.

### Echocardiography

Cardiac function was measured at baseline and at different time points by echocardiography in lightly sedated mice (100  $\mu$ L of 1 mg/mL Midazolam) using a Vevo 2100 instrument (Visualsonics, Toronto, Canada) equipped with a 30-MHz probe. Images were acquired in the 2-D mode from

short axis at the level of papillary muscles and in the parasternal long axis at a frame rate of 300 fps. A trained sonographer blinded to diet and genotype captured and analyzed the images. Only data acquired after 20 wk of dietary intervention are presented here.

### Invasive Hemodynamics

Left ventricular function was also assessed by cardiac catheterization in mice anesthetized using isoflurane anesthesia [1.5%–2% (vol/vol) maintenance]. A 1.4-Fr catheter equipped with a pressure transducer (SPR-671, Millar Instruments, Houston, TX) was guided retrogradely into the left ventricle and traces recorded using Powerlab 8/30 series (AD Instruments, Colorado Springs, CO). Data were analyzed using Labchart 8 software (AD Instruments, Colorado Springs, CO) to determine indices of contractile function. Data were acquired for a duration of 1.5–2 min and the last 10 s of the tracings were used for analysis. Left ventricular contractile parameters including developed pressure,  $dP/dt_{max}$ , and relaxation parameters including  $dP/dt_{min}$  and half-relaxation time (Tau) were determined using the blood pressure plugin available within the software package.

### Metabolic Phenotyping

Body composition was measured by nuclear magnetic resonance (NMR, model LF50, Bruker Instruments) after 16 wk of dietary intervention. Insulin sensitivity was measured by insulin tolerance test (ITT) following a 3–4-h fast, beginning at ZT3. Briefly, 0.75 U/kg of humulin-R100 (Eli Lilly, Indianapolis, IN) was injected intraperitoneally after baseline blood glucose was measured. Blood glucose measurements were made at 0, 15, 30, 60, 90, and 120 min. Data were normalized to blood glucose levels at baseline. Glucose tolerance tests (GTTs) were performed following a 6-h fast, beginning at ZT0. Glucose was injected intraperitoneally at 2 g/kg body weight and blood glucose was measured at *time* 0, 15, 30, 60, 90, and 120 min. ITTs and GTTs were performed between 16 and 18 wk after dietary intervention with a week for recovery between the two tests. Insulin ELISA (Crystal Chem, Elk Grove Village, IL) was performed on serum samples collected at 0 and 30 min of the GTT. Cardiac triglycerides in hearts harvested after the end of the diet intervention were measured using a triglyceride assay kit (Cayman Chemicals, Ann Arbor, MI).

### Mitochondrial Isolation

A total mitochondrial fraction was isolated from the interventricular septum of the myocardium. Briefly, after euthanasia, the tissue was maintained in ice-cold BiOPS buffer (7.23 mM  $K_2EGTA$ , 2.77 mM  $CaK_2EGTA$ , 20 mM imidazole, 0.5 mM DTT, 20 mM taurine, 5.7 mM ATP, 14.3 mM phosphocreatine, 6.56 mM  $MgCl_2 \cdot 6H_2O$ , 50 mM MES, pH 7.1 with KOH) until homogenization. Mitochondrial isolation was performed as previously described (35). Bradford assay was performed to determine protein concentration.

### Oxygen Consumption

Mitochondrial substrate oxidation was assessed using the Seahorse XF96 analyzer (Agilent Technologies, Santa Clara, CA). All reagents were purchased from Sigma (St. Louis, MO)

and the substrates were freshly prepared. Briefly, 2.5  $\mu$ g of cardiac mitochondria were seeded on a polyethylene terephthalate (PET) plate and centrifuged for 20 min at 2,000 g at 4°C. Substrates were added to the assay buffer at the following final concentrations: pyruvate at 2.5 mM, malate at 0.5 mM, and palmitoyl carnitine at 0.02 mM. Injections were made in the following sequential order (final concentrations): ADP (2 mM), succinate (2 mM), and cytochrome-c (6.4  $\mu$ M).

### ROS Production

Mitochondrial hydrogen peroxide emission, as a proxy for mitochondrial ROS production, was measured in isolated mitochondria using a microplate assay as previously described (36). Briefly, ROS production in state 3 was assessed in respiration assay buffer containing amplex red, superoxide dismutase, ADP at varying concentrations (10–1,000  $\mu$ M), succinate (5 mM), glutamate (10 mM), malate (2 mM), as substrates in addition to 5 mM deoxyglucose and 5 U/mL hexokinase. Deoxyglucose and hexokinase were used in a coupled reaction that uses ATP to synthesize deoxyglucose-6-phosphate and ADP, ensuring adequate ADP concentrations to facilitate mitochondrial respiration. Mitochondria (1.5–2  $\mu$ g) were added immediately before kinetic-based measurement of the accumulating fluorescent resorufin product using excitation/emission at 530 nm/590 nm in a Spectramax i3 plate reader (Molecular Devices, San Jose, CA). A standard curve using different concentrations of hydrogen peroxide (0–1,000  $\mu$ M) was performed on each plate. ROS production in *state* 4 was assessed under identical conditions in buffer supplemented with oligomycin (0.01 mg/mL).

### ATP Synthesis

ATP synthesis rates were assessed in isolated mitochondria using a fluorometer (Horiba Systems). Briefly, buffer Z lite (105 mM KMES, 30 mM KCl, 10 mM  $KH_2PO_4$ , 5 mM  $MgCl_2 \cdot 6H_2O$ , 0.5 mg/mL BSA, pH 7.4 with KOH) supplemented with glucose, hexokinase/G-6-PDH (Sigma, St. Louis, MO), Ap5a (an inhibitor of adenylate kinase, Sigma, St. Louis, MO), and NADP (Sigma, St. Louis, MO) was added to 5  $\mu$ g of mitochondria. Basal and ADP-stimulated ATP synthesis rates were measured kinetically from the formation of NADPH in a coupled reaction that uses ATP for conversion of glucose to glucose-6-phosphate (G6P) by hexokinase and subsequently to 6-phosphogluconolactone by G6P dehydrogenase coupled with reduction of NADP to NADPH. NADPH accumulation was measured by fluorometry using excitation/emission wavelengths of 345 nm/460 nm, respectively (37).

### Gene Expression

qPCR was performed using cDNA prepared from the hearts of various high-fat diet study cohorts. Changes in expression levels of different genes were measured using Power-SYBR master mix (Applied Biosystems) and custom designed primer pairs (IDT, Coralville, IA). Sequences for primer pairs are presented in Supplemental Table S2; see <https://doi.org/10.6084/m9.figshare.15050721>. Primer design was performed using Primer Blast and parameters were chosen to limit amplicon length to less than 200 bp and when possible,



primer pairs were generated to amplify from exon-exon junctions. Preliminary testing of primer pairs was performed using a generic PCR protocol and using genomic DNA and cDNA as templates, and primers that generated an amplicon from cDNA samples alone were used for qPCR (data not shown). To ensure that single amplicons were generated during qPCR, melting curves were inspected at the time of data extraction using the QuantStudio7 software (Applied Biosystems). Data were analyzed using the  $\Delta\Delta C_t$  method and expressed as fold change normalized to control diet groups with mean  $\Delta\Delta C_t$  values obtained from biological replicates of the control diet groups set as 1.

## Histology

At the time of euthanasia, a small portion of the apex was placed in zinc-formalin buffered saline fixative. Tissues were stored in the fixative until they were processed for paraffin embedding. Sections (5  $\mu$ M) were cut using a microtome and samples were processed for Masson's trichrome staining. Sections were scanned using an Ariol Slide scanner (Leica Biosystems, Buffalo Grove, IL) and processed for analysis. Quantification was performed using the open-source Fiji software.

## Statistics

Data were analyzed using Graphpad Prism v.8 software (San Diego, CA). Tests used were chosen depending on the number of groups in each experiment. Student's *t* test was used when comparing two groups and one-way ANOVA was used when comparing more than two groups to determine differences followed by post hoc analysis using Tukey's test to determine statistical significance. Repeated-measures ANOVA was used where appropriate. Statistical significance was set at  $P < 0.05$ , and data are presented as means  $\pm$  SE.

## RESULTS

### HFD Feeding Altered Systemic Metabolism but Did Not Induce Cardiac Dysfunction in GRK2 Wild-Type Mice

GRK2 is an important mediator of cardiac dysfunction in various models of heart failure (10–16). We therefore sought to determine the role of GRK2 in cardiac dysfunction associated with dysmetabolic states. Cardiomyocyte knockout of GRK2 subject to long-term fat feeding with lard-based diet beginning at 10 wk of age developed glucose intolerance and insulin resistance equivalent to wild-type animals fed HFD (Supplemental Fig. S2; see <https://doi.org/10.6084/m9.figshare.15050730>). Although some studies reported cardiac dysfunction in wild-type animals as early as 15–20 wk after feeding with lard-based HFD (30, 31), we observed no impairment in cardiac function in GRK2<sup>fl/fl</sup> mice even after 36 wk of lard-based HFD feeding. Echocardiography data suggest preserved cardiac function in GRK2 cardiomyocyte knockout animals compared with GRK2<sup>fl/fl</sup> animals fed control diet [ejection fraction (EF):  $0.82 \pm 0.01$  vs.  $0.8 \pm 0.02$ ,  $P = \text{ns}$ ] and also following HFD feeding (EF:  $0.79 \pm 0.02$  vs.  $0.8 \pm 0.01$ ,  $P = \text{ns}$ ) (Supplemental Table S3; see <https://doi.org/10.6084/m9.figshare.15050727>). Echocardiography performed at earlier time points did not indicate overt systolic dysfunction at any of these time points (12 wk and 24 wk after initiation of diets, data not shown). These findings

precluded our ability to test our initial hypothesis and led us to conduct a more detailed analysis of the adaptations of the murine heart to high-fat feeding.

### C57BL/6J Mice Are Not Susceptible to Cardiac Dysfunction following Metabolic Stress Induced by Lard-Based HFD Feeding at Either 10 or 20 wk of Age

Since background strain of animals can be an important determinant of phenotypic outcomes as reported in other models of heart disease (38–42), we investigated the effect of long-term fat feeding using lard-based high-fat diet in mice on the C57BL/6J background, a strain that is sensitive to developing obesity, insulin resistance, and diabetes when placed on a high-fat diet (43) and previously reported to develop cardiac dysfunction after long-term fat feeding (31). GRK2<sup>fl/fl</sup> animals fed lard-based HFD beginning at 9 wk of age did not develop cardiac dysfunction. We therefore determined the response of hearts from mice on the C57BL/6J background when the HFD was initiated in older animals (20 wk of age referred to as “HF<sub>L</sub> 20”) and compared these responses with animals in which the diet was initiated at 10 wk of age (referred to as “HF<sub>L</sub> 10”). HFD feeding significantly increased fat mass measured at 16 wk after diet initiation (Fig. 1A) and induced glucose intolerance and insulin resistance after 18 wk of lard-based HFD (Fig. 1, B–D). After 20 wk of HFD, transthoracic echocardiography revealed no significant alterations in cardiac function regardless of the age at which HFD feeding was initiated (EF, HF<sub>L</sub> 10–10% fat vs. 60% fat:  $0.81 \pm 0.01$  vs.  $0.78 \pm 0.02$ ,  $P = \text{ns}$ ; EF, HF<sub>L</sub> 20–10% fat vs. 60% fat:  $0.83 \pm 0.01$  vs.  $0.82 \pm 0.01$ ,  $P = \text{ns}$ , Table 1). These results were corroborated by LV catheterization studies. HFD feeding resulted in significant increases in developed pressure in both HF<sub>L</sub> 10 and HF<sub>L</sub> 20 mice, but no differences were observed in first derivatives of LV pressure between control and high-fat-fed groups in HF<sub>L</sub> 10 mice ( $dP/dt_{\text{max}}$ , 10% fat vs. 60% fat:  $6,229.18 \pm 624.92$  vs.  $6,696.54 \pm 471.4$ ,  $P = \text{ns}$ ). However, HF<sub>L</sub> 20 mice fed a high-fat diet had higher  $dP/dt_{\text{max}}$  compared with control diet (10% fat vs. 60% fat:  $5,004.54 \pm 166.81$  vs.  $6,127.27 \pm 202.23$ ,  $P < 0.01$ ) (Table 1). Taken together, these data indicate that high-fat feeding for up to 20 wk in HF<sub>L</sub> 10 mice might not impair cardiac function as reported previously (31). Moreover, HF<sub>L</sub> 20 mice fed lard-based HFD paradoxically developed increased ventricular contractility ( $dP/dt_{\text{max}}$ ), but all other parameters were similar to animals fed normal chow. Furthermore, relative to HF<sub>L</sub> 10 mice, no evidence of reduced LV function by echocardiography or LV catheterization was observed in HF<sub>L</sub> 20.

### Saturated Fat-Rich Diet Does Not Induce Cardiac Dysfunction in C57BL/6J Mice

Saturated fat intake has been associated with increased risk of coronary heart disease although it has been debated in the recent years (44–46). Saturated fatty acids such as palmitate induce a robust apoptotic effect in vitro that is rescued by addition of unsaturated fatty acids such as oleic acid (47, 48). Since lard is a combination of saturated and unsaturated fat (Supplemental Table S1), we assessed whether feeding a diet rich in saturated fat impairs cardiac function in mice and whether this response may be affected by age. About 10-wk-old (referred to as “HF<sub>S</sub> 10”) and 20-wk-old

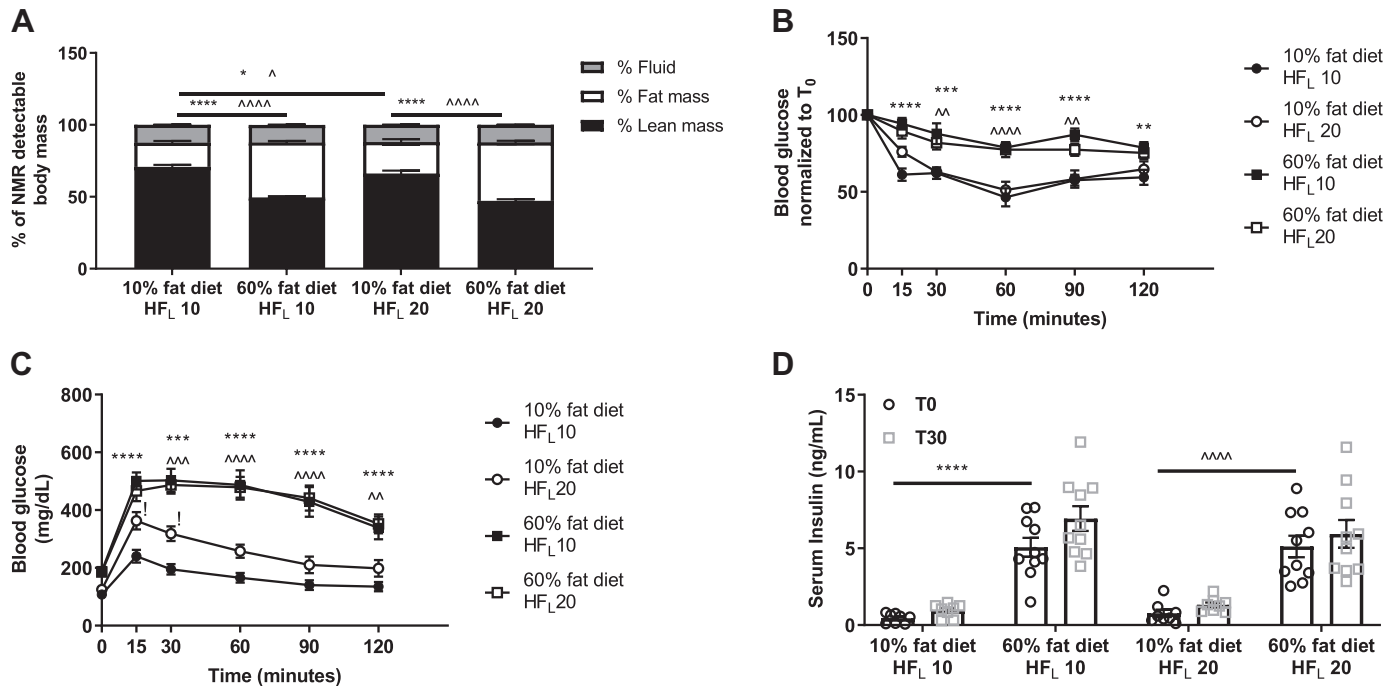


**Figure 1.** Metabolic phenotyping of mice fed lard-based diets. **A:** body mass composition as determined by NMR; **B:** insulin sensitivity assessed by insulin tolerance test (ITT); **C:** results from intraperitoneal glucose tolerance tests (IPGTT); **D:** serum concentrations of insulin measured by ELISA in the fasting state (T0) and the 30-min time point (T30) of the IPGTT. Data are means  $\pm$  SE and were analyzed by repeated-measures two-way ANOVA followed by post hoc analysis using Tukey's test. Statistical significance was set at  $P < 0.05$  ( $n > 6$  animals/group). HF<sub>L</sub> 10 and HF<sub>L</sub> 20 refer to mice that were 10 wk of age or 20 wk of age, respectively, at the time of initiation with lard-based diets (for **A**: \*,  $^{\wedge}P < 0.05$ , \*\*\*\*,  $^{\wedge\wedge\wedge\wedge}P < 0.0001$ , \*significance for lean mass,  $^{\wedge}$ significance for fat mass; for **B**, **C**, and **D**: \*\*,  $^{\wedge}P < 0.01$ , \*\*\*,  $^{\wedge\wedge\wedge}P < 0.001$ , \*\*\*\*,  $^{\wedge\wedge\wedge\wedge}P < 0.0001$ ; \* $P < 0.05$  10% diet HF<sub>L</sub> 10 vs. 60% diet HF<sub>L</sub> 10;  $^{\wedge}P < 0.05$  10% diet HF<sub>L</sub> 20 vs. 60% diet HF<sub>L</sub> 20,  $^{\wedge}P < 0.05$  10% diet HF<sub>L</sub> 10 vs. 10% diet HF<sub>L</sub> 20).

(referred to as “HF<sub>S</sub> 20”) mice fed a diet rich in saturated fat (58% calories) and sucrose (19% calories) (HFHS) had significantly higher fat mass by 16 wk after dietary intervention (Fig. 2A) and developed glucose intolerance and insulin resistance relative to mice fed a low-fat high-sucrose (LFHS) or low-fat low-sucrose (LFLS) diet (Fig. 2, B–F). Age-related differences in the systemic response to increasing dietary sucrose were observed. HF<sub>S</sub> 20 animals fed LFHS diet had an intermediate increase in fat mass, relative to HFHS, but developed glucose intolerance that was comparable to animals fed HFHS diet (Fig. 2, A and E). Cardiac function as assessed using transthoracic echocardiography revealed no impairment in function in the high-fat group compared with the low-fat groups in both HF<sub>S</sub> 10 (EF, LFLS:  $0.84 \pm 0.01$ , LFHS:  $0.85 \pm 0.01$  and HFHS:  $0.78 \pm 0.04$ ,  $P = \text{ns}$ ) as well as HF<sub>S</sub> 20 groups (EF, LFLS:  $0.85 \pm 0.01$ , LFHS:  $0.85 \pm 0.01$  and HFHS:  $0.81 \pm 0.02$ ,  $P = \text{ns}$ ) (Table 1). Analysis of cardiac function using LV catheterization in HF<sub>S</sub> 10 mice revealed no significant changes in first derivatives of LV pressures consistent with preserved systolic function ( $\text{dp}/\text{dt}_{\text{max}}$ , LFLS:  $6531.73 \pm 1089.22$ , LFHS:  $5744.71 \pm 154.7$  and HFHS:  $7062.11 \pm 425.61$ ,  $P = \text{ns}$ , Table 1). Technical limitations precluded collection of invasive hemodynamics data from animals initiated with saturated fat diet at 20 wk of age. Taken together, cardiac function was not impaired following long-term fat feeding in animals regardless of the saturated fat content or age at the time of initiation.

### High-Fat Feeding Induced Cardiac Hypertrophy without Cardiac Fibrosis or Diastolic Dysfunction

Although cardiac function was not impaired with high-fat feeding, HF<sub>L</sub> 10 mice but not HF<sub>L</sub> 20 mice developed significant cardiac hypertrophy. On the saturated fat diet, cardiac hypertrophy developed in HF<sub>S</sub> 10 and HF<sub>S</sub> 20 animals on HFHS diet, although the increase in heart weight was greater in HF<sub>S</sub> 10 mice (Table 2). Cardiac fibrosis was not evident following quantification of trichrome-stained cardiac sections prepared from the various age and fat-fed groups (Supplemental Fig. S3; see <https://doi.org/10.6084/m9.figshare.15050724>). Lack of cardiac fibrosis, equivalent  $\text{dp}/\text{dt}_{\text{min}}$ , end-diastolic pressures, and relaxation half times ( $\tau$ ) in all the groups tested (Table 1) support the absence of significant diastolic abnormalities following high-fat feeding in these mice.

### Younger Mice but Not Older Mice Exhibit Triglyceride Accumulation upon HFD Feeding

Accumulation of lipid species such as triglycerides, diacylglycerol and ceramides in the heart has been suggested to contribute to diabetic cardiomyopathy (49, 50). We therefore tested whether high-fat feeding in mice resulted in lipid accumulation and observed a small but significant increase in cardiac triglycerides in HF<sub>L</sub> 10 and HF<sub>S</sub> 10 mice fed high-fat diets ( $\mu\text{g}/\text{mg}$  tissue weight, 10% fat diet:  $3.77 \pm 0.16$  versus 60% fat diet:  $4.56 \pm 0.28$ ,  $P < 0.05$ ; LFLS:  $2.81 \pm 0.43$ , LFHS:

**Table 1.** Assessment of cardiac function in vivo using echocardiography and invasive left ventricular hemodynamics in mice subject to dietary intervention

	HF <sub>L</sub> 10			HF <sub>L</sub> 20			HF <sub>S</sub> 10			HF <sub>S</sub> 20		
	10% Fat	60% Fat	10% Fat	60% Fat	10% Fat	60% Fat	LFLS	LFHS	HFHS	LFLS	LFHS	HFHS
Ejection fraction	0.81±0.01	0.78±0.02	0.83±0.01	0.82±0.01	0.84±0.01	0.85±0.01	0.85±0.01	0.85±0.01	0.78±0.04	0.85±0.01	0.85±0.01	0.81±0.02
Heart rate, beats/min	653±24	630±23	658±11	609±31	725±11	728±21	725±11	728±21	681±19	664±19	664±19	659±16
LV mass estimated, mg	59.34±3.39	67.24±2.28*	83.21±3.77	81.73±5.29	92.62±4.4	81.47±4.02	92.62±4.4	81.47±4.02	87.06±4.52	73.73±3.77	73.73±3.77	94.85±3.94
End-systolic volume estimated, $\mu$ L	4.27±0.33	5.19±0.74	5.26±0.37	5.33±0.53	5.49±0.38	5.03±0.5	5.49±0.38	5.03±0.5	9.76±2.01	4.86±0.52	4.86±0.52	6.62±0.79
End-diastolic volume estimated, $\mu$ L	23.95±1.36	29.7±2.71	36.63±2.38	34.75±3.12	35.38±2.29	32.64±2.67	35.38±2.29	32.64±2.67	44.59±3.97	32.85±2.72	32.85±2.72	34.75±2.97
EDV/LV mass	0.41±0.02	0.44±0.03	0.44±0.02	0.42±0.02	0.38±0.01	0.4±0.02	0.38±0.01	0.4±0.02	0.52±0.04	0.39±0.03	0.37±0.02	0.37±0.03
Developed Pressure, mmHg	104.33±2.55	117.26±5.77*	84.97±5.1	105.69±5.13*	89.73±6.4	96.33±5	89.73±6.4	96.33±5	97.5±4.67			
Heart rate, beats/min	414.95±22.1	402.96±24.01	425.43±26.11	419.84±39.37	456.11±39.26	431.3±31.34	456.11±39.26	431.3±31.34	472.03±25.13			
dP/dt <sub>max</sub> , mmHg/s	6,229.2±624.9	6,696.5±471.4	5,004.5±166.8	6,127.3±202.2**	6,531.7±1089.2	5,744.7±154.7	6,531.7±1089.2	5,744.7±154.7	7,062.1±425.6			
dP/dt <sub>min</sub> , mmHg/s	-6,756.4±643.7	-6,373.5±340.1	-5,132.3±327.1	-5,882±148.4	-6,684.7±1256	-5,883.2±690.6	-6,684.7±1256	-5,883.2±690.6	-7,165.1±363.9			
EDP, mmHg	3.02±3.1	3.08±2.2	7.63±2.2	6.19±2.7	7.13±1.36	5.57±0.88	7.13±1.36	5.57±0.88	10.08±2.99			
Tau, s	0.014±0.001	0.014±0.001	0.018±0.004	0.018±0.002	0.013±0.003	0.012±0.001	0.013±0.003	0.012±0.001	0.015±0.003			

Values are means  $\pm$  SE. Composition of the diets is described in Supplemental Table S1. HF<sub>L</sub> 10 and HF<sub>L</sub> 20 refer to mice that were 10 or 20 wk of age, respectively, at the time of initiation with lard-based diets. HF<sub>S</sub> 10 and HF<sub>S</sub> 20 refer to mice that were 10 or 20 wk of age, respectively, at the time of initiation with saturated fat-based diets. dP/dt<sub>max</sub> and dP/dt<sub>min</sub>, maximum and minimum first derivative of LV pressure, respectively; EDP, end-diastolic pressure; EDV, end-diastolic volume; LFLS, low-fat low-sucrose; LFHS, low-fat high-sucrose; HFHS, high-fat high-sucrose; LV, left ventricular. Statistical testing was performed within age groups. Within age group data were analyzed by Student's *t* test for HF<sub>L</sub> 10, and HF<sub>L</sub> 20, and by one-way ANOVA for HF<sub>S</sub> 10, and HF<sub>S</sub> 20. \**P* < 0.05, \*\**P* < 0.01 for comparisons within HF<sub>L</sub> 10 and HF<sub>L</sub> 20.

2.85±0.26 and HFHS: 4.18±0.37, *P* < 0.05). Similarly, increases in cardiac triglycerides were not evident in HF<sub>L</sub> 20 and HF<sub>S</sub> 20 mice fed the high-fat diets (Table 2).

### HFD Feeding Does Not Induce Mitochondrial Dysfunction Regardless of Saturated Fat Content

Mitochondrial dysfunction has been described in cardiomyopathy associated with diabetes and obesity (51–54). We therefore assessed mitochondrial oxygen consumption rates (OCR) in isolated cardiac mitochondria from mice fed HFD (both saturated fat-rich and lard-based diets) using the Seahorse Flux Analyzer. Lard-based HFD feeding did not cause significant alterations in ADP-stimulated oxygen consumption rates in isolated cardiac mitochondria with pyruvate- or palmitoyl carnitine-malate as substrates (Table 3). There also was no difference in ADP-stimulated oxygen consumption rates in isolated cardiac mitochondria from HF<sub>S</sub> 10 mice regardless of the substrates used (Table 3). Seahorse-based OCR was not determined in HF<sub>S</sub> 20 animals secondary to technical limitations. ATP synthesis rates were measured to determine whether comparable oxygen consumption rates represented coupled or uncoupled respiration in the high-fat diet-fed groups. ATP synthesis rates in cardiac mitochondria were not significantly different between control and HFD-fed groups (both lard-based and saturated fat-based) using pyruvate-malate as substrates (Table 3). Similarly, ATP synthesis rates in isolated cardiac mitochondria from lard-based diet using PC-malate as substrates were not significantly different between the 10% fat and 60% fat-fed groups (Table 3). In cardiac mitochondria from HF<sub>S</sub> 20 animals, a significant increase in ATP synthesis rate in LFHS group (*P* < 0.01, by one-way ANOVA) using PC-malate as substrates was observed (Table 3). These measurements were not carried out in HF<sub>S</sub> 10 animals fed saturated fat-based diet given cardiac mitochondrial sample limitations. We further assessed whether isolated cardiac mitochondria from HF<sub>L</sub> 10, HF<sub>L</sub> 20, HF<sub>S</sub> 10, and HF<sub>S</sub> 20 mice had differences in generation of reactive oxygen species, specifically hydrogen peroxide (H<sub>2</sub>O<sub>2</sub>). There were no significant differences in rates of generation of H<sub>2</sub>O<sub>2</sub> in isolated mitochondria (Table 4). Taken together, these results suggest that regardless of the degree of saturation of fatty acids, 20 wk of high-fat diet feeding in younger and older mice did not induce mitochondrial dysfunction or ROS overproduction.

### HFD Feeding Induces Modest Increases in Extracellular Matrix Remodeling-Related Genes

Because HFD reproducibly caused hypertrophy across multiple cohorts without cardiac dysfunction, we sought to determine if the hypertrophy observed was associated with transcriptional changes characteristic of pathological hypertrophy and cardiac fibrosis (Table 5). ANP levels in the 60% fat diet group were significantly decreased in HF<sub>L</sub> 20 animals and unchanged in HF<sub>L</sub> 10 animals. In the HF<sub>S</sub> 10 and HF<sub>S</sub> 20 groups, animals fed HFHS diet showed a decrease in ANP, although the changes are not statistically significant. Regardless of the saturated fat content of the diet, there were no significant differences in BNP in the hearts of fat-fed groups compared with their respective controls. A modest increase in Myh7 was apparent in 60% fat-fed animals



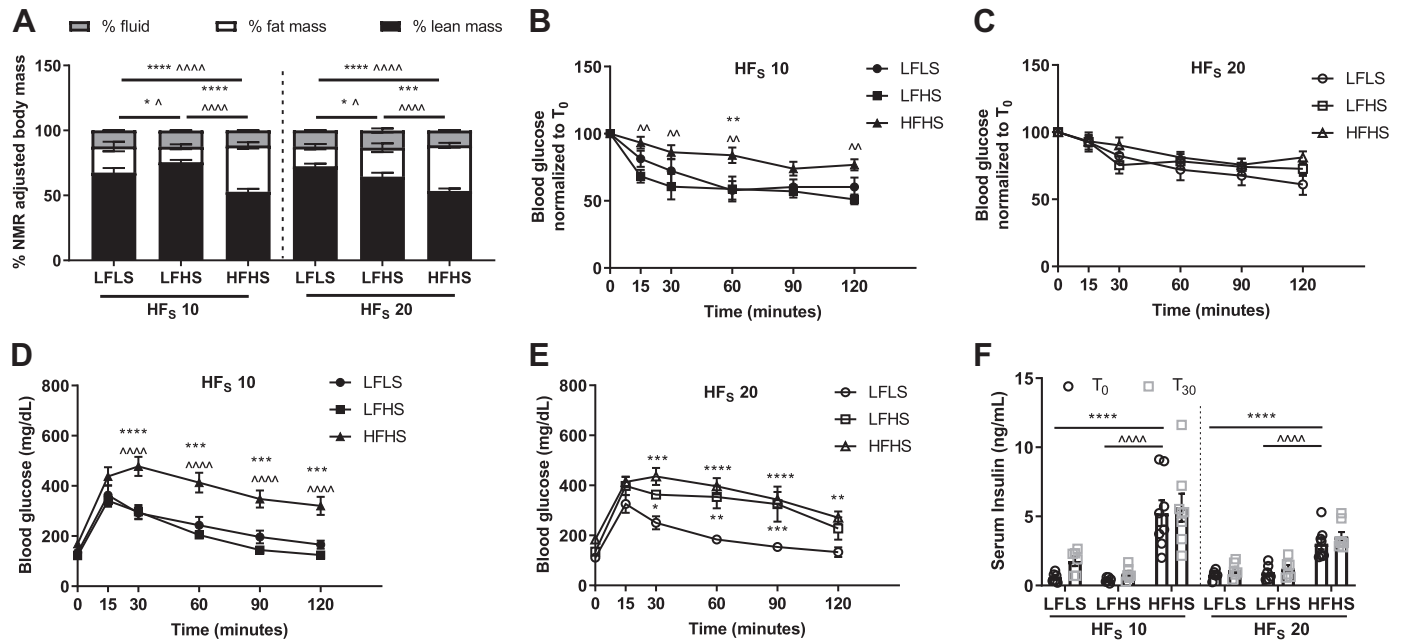


**Figure 2.** Metabolic phenotyping of mice fed saturated fat-based diets. A: body mass composition determined by NMR; B and C: insulin sensitivity assessed by insulin tolerance test (ITT); D and E: results from intraperitoneal glucose tolerance tests (IPGTT); F: serum concentrations of insulin measured by ELISA in the fasting state (T<sub>0</sub>) and the 30-min time point (T<sub>30</sub>) of the IPGTT. Data are means  $\pm$  SE and were analyzed by repeated measures two-way ANOVA followed by post hoc analysis using Tukey's test. Only within age group comparisons were performed. Statistical significance was set at  $P < 0.05$  ( $n > 6$  animals/group). HF<sub>S</sub> 10 and HF<sub>S</sub> 20 refer to mice that were 10 wk of age or 20 wk of age, respectively, at the time of initiation with saturated fat-based diets. (\*,  $^{\wedge}P < 0.05$ , \*\*\*  $P < 0.001$ , \*\*\*\*  $P < 0.0001$ , \*significance for lean mass,  $^{\wedge}$ significance for fat mass; for B, C, D, and E: \*\*,  $^{\wedge}P < 0.01$ , \*\*\*  $P < 0.001$ , \*\*\*\*  $P < 0.0001$ ; \*vs. LFLS;  $^{\wedge}$ vs. LFHS). HFHS, high-fat high-sucrose; LFLS, low-fat low-sucrose; LFHS, low-fat high-sucrose.

compared with the control diet within the HF<sub>L</sub> 20 group. Modest increases in collagen transcripts and matrix metalloproteinases (MMP2 and MMP9) were evident in high-fat diet groups regardless of saturated fat content or age of the mice. Taken together, high-fat feeding regardless of the fatty acid saturation did not induce large differences in genes that are characteristic of pathological hypertrophy but could be activating matrix remodeling.

### HFD Feeding Increases the Expression of Fatty Acid Metabolism-Related Genes

Since HFD feeding increased triglyceride accumulation in the heart independent of impaired systolic function, we sought to determine if metabolic adaptations in the heart could have limited free fatty acid accumulation and lipotoxicity. Expression levels of genes involved in fatty acid uptake, triglyceride formation, and fatty acid oxidation (FAO) were measured (Table 5). Myocardial expression of the fatty acid importer CD36 was significantly induced, whereas expression levels of Dgat1, the enzyme catalyzing the rate limiting step in TAG synthesis, were not altered by chronic fat feeding. Long-term fat feeding significantly increased mRNA levels of Plin5, the gene product of which regulates lipid droplet formation and breakdown. Expression of Cpt1b and Acs1L was increased. AcadL expression was increased in both HF<sub>L</sub> 10 and HF<sub>L</sub> 20 animals on 60% fat diet. In both younger and older mice, mRNA levels of Hadh and Pnpla2 were increased when fed a lard-based diet but decreased when fed a saturated fat-rich diet. Expression levels of mRNA for Pdk4 exhibited the most robust increase. Taken together, these data are consistent with an increased fatty acid uptake and oxidation and

reduced pyruvate oxidation in response to HFD. Increased FAO has been linked to increased ROS generation in mitochondria that may activate mitochondrial uncoupling. Consistent with prior observations by our group and others (51, 55) uncoupling protein 3 expression (Ucp3) was induced following high-fat feeding regardless of degree of fatty acid saturation or age at HFD initiation. As no differences in mitochondrial ROS synthesis rates were observed in isolated mitochondria between control and high-fat-fed mice (Table 4), we examined other antioxidant defense mechanisms. Catalase expression was significantly increased by HFD independent of the type of diet and age at time of initiation with HFD. However, expression levels of SOD-2 and HO-1 were unchanged (Table 5).

## DISCUSSION

A distinct cardiomyopathy associated with diabetes and obesity has been suggested as a precursor to heart failure but the mechanisms that contribute to development of cardiomyopathy in diabetes and obesity are not completely understood. Several potential mechanisms have been suggested including lipotoxicity, mitochondrial dysfunction, and oxidative stress (56, 57). In line with these suggested mechanisms, multiple approaches to model cardiac dysfunction in diabetes and obesity have been reported in the literature. Animals with cardiomyocyte-restricted transgenes for example, (28, 29) might only partially model cardiomyopathy of dysmetabolic states. Specifically, they do not account for systemic perturbations in metabolism, which has been hypothesized to directly contribute to cardiac

**Table 2.** Body mass at the time of euthanasia, cardiac hypertrophy as measured by HW normalized to TL and cardiac TG content in mice subject to dietary intervention

	Body Mass, g	HW/TL, mg/mm	Cardiac TG, $\mu$ g/mg Wet wt
HF <sub>L</sub> 10			
10% fat	31.1 $\pm$ 0.8	8.4 $\pm$ 0.32	3.77 $\pm$ 0.16
60% fat	54.8 $\pm$ 1.3****	10.77 $\pm$ 0.5***	4.56 $\pm$ 0.28*
HF <sub>L</sub> 20			
10% fat	33.8 $\pm$ 1.2	8.84 $\pm$ 0.35	3.43 $\pm$ 0.24
60% fat	53.9 $\pm$ 1****	9.66 $\pm$ 0.25	3.95 $\pm$ 0.24
HF <sub>S</sub> 10			
LFLS	35.3 $\pm$ 0.8	9.01 $\pm$ 0.37	2.81 $\pm$ 0.43
LFHS	32.7 $\pm$ 0.9	8.98 $\pm$ 0.13	2.85 $\pm$ 0.26
HFHS	53.2 $\pm$ 1.7****,!!!!	10.26 $\pm$ 0.27^,!	4.18 $\pm$ 0.37^,!
HF <sub>S</sub> 20			
LFLS	35.2 $\pm$ 0.8	9.22 $\pm$ 0.11	3.53 $\pm$ 0.23
LFHS	33.5 $\pm$ 3	7.98 $\pm$ 0.52	3.97 $\pm$ 0.31
HFHS	52.7 $\pm$ 1****,!!	9.74 $\pm$ 0.24!!!	5 $\pm$ 0.74

Values are means  $\pm$  SE. Composition of the diets is described in Supplemental Table S1. Statistical testing was performed within each age group. Statistical significance was set at  $P < 0.05$ . HF<sub>L</sub> 10 and HF<sub>L</sub> 20 refer to mice that were 10 wk of age or 20 wk of age, respectively, at the time of initiation with lard-based diets. HF<sub>S</sub> 10 and HF<sub>S</sub> 20 refer to mice that were 10 wk of age or 20 wk of age, respectively, at the time of initiation with saturated fat-based diets. HFHS, high-fat high-sucrose; HW, heart weight; LFHS, low-fat high-sucrose; LFLS, low-fat low-sucrose; TG, triglyceride; TL, tibia length. \* $P < 0.05$ , \*\*\* $P < 0.001$ , and \*\*\*\* $P < 0.0001$ , 10% fat vs. 60% fat ( $n > 6$  animals/group). ^ $P < 0.05$  and \*\*\*\* $P < 0.0001$ , LFLS vs. HFHS. ! $P < 0.05$ , !! $P < 0.01$ , !!! $P < 0.001$ , and !!!! $P < 0.0001$ , LFHS vs. HFHS ( $n \geq 6$  animals/group).

dysfunction in diabetes and obesity. A widely used model to study the course of development of cardiac disease in these dysmetabolic states is the long-term high-fat feeding model, where impairment in contractile function has been reported to become apparent over time (31). In this study, we initially sought to understand the role of GRK2 in cardiac dysfunction associated with diabetes and obesity. GRK2 has previously been implicated as a critical mediator of cardiac dysfunction in diverse models of heart failure (10, 11, 13, 14). Heterozygous germline GRK2-deficient mice fed a high-fat diet showed lower cardiac lipid accumulation and a lower induction of maladaptive remodeling associated genes (17, 58), suggesting GRK2 may promote cardiac dysfunction in cardiomyopathy associated with dysmetabolic states. Since GRK2 loss protects from diet-induced obesity (59), the protective cardiac effects afforded by reduced GRK2 expression reported in the heterozygous animals could be secondary to improved whole body metabolism. This model does not identify the cell type that mediates this effect, such as the cardiomyocytes versus fibroblasts. We therefore asked whether reducing GRK2 in cardiomyocytes prevents cardiac dysfunction induced by long-term fat feeding. However, failure to uncover a cardiac phenotype by echocardiography in wild-type animals despite using previously reported dietary regimens (31, 60, 61) motivated us to thoroughly characterize the reproducibility and utility of this diet-induced obesity model for diabetic cardiomyopathy. The GRK2 animals used in our studies were on a mixed background and since strain background can affect phenotypes

(38–42), we used the C57BL/6J mouse strain for characterizing the cardiac phenotype in response to long term high-fat feeding. We focused on this strain given its susceptibility to diet-induced obesity, the widespread use of this strain for metabolic studies (62) and previous characterization of cardiac dysfunction induced by high-fat feeding in this model. Our results suggest that long-term high-fat feeding in mice might not be a reproducible model to understand the cardiomyopathy related to diabetes and obesity. This raises the possibility that additional ill-defined environmental factors could potentially contribute to development of a cardiac phenotype with fat feeding that has been reported by other groups. Some differences pertinent to the technical aspects of echocardiography are important to consider in light of these conflicting data. In our study, data were acquired in 2-D mode, which estimates cardiac function based on parameters obtained in transverse and parasternal long axis to reflect global left ventricular function. A number of studies (31, 53, 61, 63–67) examining the long-term high-fat feeding model have used M-mode echocardiography which estimates left ventricular function based on parameters acquired from wall motion on a defined time scale. This mode of echocardiography extrapolates global left ventricular function based on what is observed from changes in LV chamber dimensions in one dimension during systole and diastole (68). Despite these differences, a study that used both M-mode and 2-D echocardiography also reported absence of cardiac dysfunction following long-term high-fat feeding (32).

Since a lard-based high-fat diet did not induce contractile dysfunction as assessed by echocardiography and LV catheterization, we sought to determine if fatty acid composition could influence the development of cardiac dysfunction. Lard-based diets have a saturated fat content that approximates to 20% total calories and the remaining 40% calories in a lard-based high-fat diet are contributed by unsaturated fatty acids (see Supplemental Table S1). Previous studies have shown in cell culture models that unsaturated fatty acids such as oleate can rescue the apoptotic effect of excess saturated fatty acids such as palmitate (47, 48). To address the possibility that high amounts of unsaturated fatty acids in lard-based diets could potentially protect cardiomyocytes from detrimental effects of saturated fatty acids, we developed a formulation that was enriched with saturated fat (up to 95% of total fatty acids). When fed this formulation which was also enriched with sucrose (19% of total calories), mice developed insulin resistance and were glucose intolerant by 16–18 wk. Periodic assessment of cardiac function by echocardiography revealed preserved systolic function. Invasive hemodynamics revealed no differences in first derivatives of developed pressure, indicating preserved systolic function and further corroborated the findings from echocardiography. In addition, the absence of significant differences in  $dp/dt_{min}$  suggest that relaxation may not be impaired, although these data need to be interpreted with some caution as  $dp/dt_{max}$  and  $dp/dt_{min}$  are both load-dependent parameters that are affected by changes in filling volume.

To test the possibility that age at the time of induction with high-fat diet may alter cardiac function of high-fat-fed



**Table 3. Mitochondrial function and ATP synthesis rates**

	HF <sub>L</sub> 10			HF <sub>L</sub> 20			HF <sub>S</sub> 10			HF <sub>S</sub> 20		
	10% Fat	60% Fat		10% Fat	60% Fat		LFLS	HFHS		LFLS	HFHS	
Pyr-Malate + ADP + Succinate + Cytochrome-c	80.56 ± 17.12	103.98 ± 31.67	85.24 ± 2.28	77.09 ± 16.33	113.2 ± 10.32	122.75 ± 9.73	113.2 ± 10.32	122.75 ± 9.73	87.01 ± 4.53			
	330.12 ± 91.7	313.42 ± 70.19	292.25 ± 8.83	262.75 ± 46.83	423.54 ± 31.37	417.75 ± 24.61	423.54 ± 31.37	417.75 ± 24.61	346.01 ± 54.37			
	339.3 ± 24.33	348.87 ± 55.39	353.9 ± 18.05	399.47 ± 104.38	317.05 ± 14.29	297.61 ± 25.28	317.05 ± 14.29	297.61 ± 25.28	319.55 ± 7.22			
	282.92 ± 12.34	275.37 ± 25.22	287.7 ± 9.36	316.77 ± 70.77	277.75 ± 14.56	257.38 ± 19.95	277.75 ± 14.56	257.38 ± 19.95	270.25 ± 5.38			
PC-Malate + ADP + Succinate + Cytochrome-c	74.03 ± 11.43	82.7 ± 21.5	68.88 ± 2.45	66.2 ± 16.16	91.34 ± 5.11	98.18 ± 9.13	91.34 ± 5.11	98.18 ± 9.13	82.27 ± 6.7			
	157.49 ± 23.5	205.39 ± 53.27	249.39 ± 59.55	185.64 ± 18.9	212.47 ± 33.67	215.16 ± 15.12	212.47 ± 33.67	215.16 ± 15.12	206.38 ± 40.05			
	486.73 ± 55.44	440.1 ± 60.29	431.21 ± 23.06	413.47 ± 58.7	450.08 ± 59.08	402.54 ± 72.75	450.08 ± 59.08	402.54 ± 72.75	427.87 ± 33.51			
	360.2 ± 50.53	310 ± 54.29	328.32 ± 16.51	351.48 ± 42.74	328.56 ± 29.09	330.54 ± 53.59	328.56 ± 29.09	330.54 ± 53.59	323.13 ± 18.89			
ATP synthesis rate, pmol/μg/min												
Pyr-Mal Basal 75 μM PC-Mal Basal 75 μM 2 mM	59.38 ± 15.74	50.21 ± 11.03	97.27 ± 8.3	80.19 ± 3.69	84.98 ± 3.47	87.59 ± 7.29	84.98 ± 3.47	87.59 ± 7.29	82.02 ± 3.69	112.81 ± 10.04	114.62 ± 16.62	108.44 ± 11
	270.26 ± 46.64	228.68 ± 33.41	367.49 ± 46.91	263 ± 91.15	549.4 ± 58.39	414.35 ± 104.74	549.4 ± 58.39	414.35 ± 104.74	488.22 ± 35.06	440.84 ± 75.61	419.34 ± 11.93	392.35 ± 19.55
	65.08 ± 0.77	59.87 ± 5.13	64.62 ± 2.07	63.36 ± 1.55					64.01 ± 1.39	63.5 ± 1.09	65.54 ± 1.66	
	75.49 ± 7.76	76 ± 1.82	71.41 ± 3.08	78.75 ± 0.88					69.57 ± 1.43	86.68 ± 16.2	68.14 ± 2.3	
	120.25 ± 26.24	134.67 ± 19.6	141.43 ± 18.77	124.65 ± 24.32					112.48 ± 3.97	156.01 ± 27.99 <sup>^^</sup>	117.62 ± 20.59	

Values are means ± SE. Composition of the diets is described in Supplemental Table S1. Mitochondrial function measured using the Seahorse flux analyzer in heart mitochondria isolated from mice subject to dietary intervention, and ATP synthesis rates measured in isolated heart mitochondria using fluorimetry using pyruvate-malate (Pyr-Mal) or palmitoyl carnitine-malate (PC-Mal) as substrates. HF<sub>L</sub> 10 and HF<sub>L</sub> 20 refer to mice that were 10 wk of age or 20 wk of age, respectively, at the time of initiation with lard-based diets. HF<sub>S</sub> 10 and HF<sub>S</sub> 20 refer to mice that were 10 wk of age or 20 wk of age, respectively, at the time of initiation with saturated fat-based diets. HFHS, high-fat high-sucrose; LFLS, low-fat high-sucrose; LFLS, low-fat low-sucrose. Statistical testing was performed within each age group. Data were analyzed by *t* test for comparisons in mice fed lard-based diet and by one-way ANOVA followed by post hoc analysis using Tukey's test in mice fed saturated fat-rich diet. <sup>^^</sup>*P* < 0.01 vs. LFLS (*n* > 4 animals/group).

**Table 4.**  $H_2O_2$  emission rates in mitochondria isolated from hearts of mice subject to 20 wk of dietary intervention in states 3 and 4 in the presence of oligomycin

	Substrates Only	Substrates + 5 $\mu$ M ADP	Substrates + 10 $\mu$ M ADP	Substrates + 1,000 $\mu$ M ADP
$H_2O_2$ emission rates (pmol/min/mg) in state 3 respiration				
HF <sub>L</sub> 10				
10% fat	1,529.8 ± 322.6	1,252.2 ± 279.5	646.7 ± 129.3	551.8 ± 108.9
60% fat	1,453.4 ± 390.2	1,237.3 ± 311.2	616.1 ± 186.7	1,209.6 ± 753.8
HF <sub>L</sub> 20				
10% fat	1,865 ± 539.1	1,840.4 ± 628.4	1,799.4 ± 453.9	1,872.1 ± 612.8
60% fat	2,520.9 ± 466.2	2,014.1 ± 471.1	1,710.2 ± 524.8	1,677.9 ± 418.7
HF <sub>S</sub> 10				
LFLS	1,224.7 ± 113	974 ± 278.4	696.2 ± 270.4	414.8 ± 61.7
LFHS	1,351.9 ± 173.9	732.7 ± 116.5	545.3 ± 114	696 ± 338.4
HFHS	1,633.6 ± 175.9	890.1 ± 129.7	503.6 ± 119.8	370.9 ± 78.9
HF <sub>S</sub> 20				
LFLS	2,013.2 ± 266.3	1,613.9 ± 316.1	782.4 ± 71.7	327.4 ± 368.4
LFHS	2,660.4 ± 615.8	1,139.3 ± 71.6	669.5 ± 61.8	786.8 ± 85.4
HFHS	2,436.5 ± 404.7	1,496 ± 209.8	730 ± 65.6	722.5 ± 90.1
$H_2O_2$ emission rates (pmol/min/mg) in state 4 respiration				
HF <sub>L</sub> 10				
10% fat	2,550.4 ± 380.4	2,485.6 ± 348.3	2,647.4 ± 326.7	3,078.7 ± 643.4
60% fat	2,309.3 ± 317	2,501.1 ± 378.4	2,705.4 ± 479.3	2,996.7 ± 558.2
HF <sub>L</sub> 20				
10% fat	3,680.3 ± 1,349.6	4,023.4 ± 1,748.2	3,587 ± 1,124.1	5,189.1 ± 1,291.7
60% fat	3,804.3 ± 943	3,834.8 ± 811.8	3,519 ± 480.7	5,730.2 ± 1,279.7
HF <sub>S</sub> 10				
LFLS	2,571.1 ± 91.5	2,530.2 ± 185.5	2,147.4 ± 310.3	2,729.8 ± 322
LFHS	2,373.7 ± 158.7	2,435.9 ± 222.3	2,231.3 ± 187.9	2,642.1 ± 163.1
HFHS	2,600.9 ± 174.9	2,642.9 ± 319.5	2,623.1 ± 274.8	2,789.3 ± 231.1
HF <sub>S</sub> 20				
LFLS	3,889.4 ± 472.9	3,515.8 ± 467.3	3,550.8 ± 431.9	3,948 ± 798.9
LFHS	3,031.8 ± 417.3	3,010.2 ± 478.6	3,339.1 ± 411.7	3,654.8 ± 353.7
HFHS	3,720.4 ± 382.8	3,611 ± 314.9	3,374 ± 295.4	3,362.6 ± 463.2

Values are means ± SE. Statistical testing was performed within each age group. HF<sub>L</sub> 10 and HF<sub>L</sub> 20 refer to mice that were 10 wk of age or 20 wk of age, respectively, at the time of initiation with lard-based diets. HF<sub>S</sub> 10 and HF<sub>S</sub> 20 refer to mice that were 10 wk of age or 20 wk of age, respectively, at the time of initiation with saturated fat-based diets. HFHS, high-fat high-sucrose; LFHS, low-fat high-sucrose; LFLS, low-fat low-sucrose. Multiple *t* tests were performed for determining effect of diet on mitochondrial function within each age group fed lard-based diet. Data were analyzed by one-way ANOVA followed by post hoc analysis using Tukey's test within each age group at each ADP concentration for saturated fat-fed groups ( $n \geq 3$  animals/group). No significant differences were found.

mice, we compared the older mice (20 wk old at diet initiation) with the younger mice (10 wk old at diet initiation) after 20 wk of HFD. Cardiac function as assessed by echocardiography was not significantly different between the control and high-fat groups. LV catheterization of the younger animals at the time of euthanasia suggested normal cardiac function that was comparable to that of the control groups. Other studies in mice and rats have used a cocoa-butter-based diet, which is rich in saturated fatty acids such as palmitate and stearate. These studies were conducted for 8–16 wk and the diet used did not cause obesity or insulin resistance. These studies also reported a lack of cardiac dysfunction by feeding the diet alone (69–71). In addition, under conditions of additional myocardial stress such as pressure overload or myocardial infarction, the cocoa-butter-rich diet produced beneficial effects or no effects on cardiac function (69, 72–76). In this study, the saturated fat-rich diet used is a mixture of medium chain and long chain fatty acids (Table 1) and feeding mice with the customized diet resulted in insulin resistance and obesity. This observation of an equivalently perturbed metabolic state established the context for us to investigate the effects of feeding excessive amounts of saturated fat on cardiac function in dysmetabolic states. Despite the metabolic perturbations, there was no apparent cardiac dysfunction as assessed by echocardiography or LV

catheterization emphasizing the resilience of these mouse hearts to development of cardiac dysfunction in the face of persistent metabolic stress.

We assessed cardiac steatosis, mitochondrial function, and reactive oxygen species production rates to determine whether changes in any of these parameters as previously reported in literature (54, 77, 78) were induced by high-fat feeding in our cohorts. Strikingly, we observed modest but significant increases in cardiac triglyceride content in younger groups fed with both saturated fat-rich diet and lard-based HFDs, whereas the older animals fed with either of the two high-fat diets did not increase their triglyceride content. Mitochondrial dysfunction has been described in genetic and diet-induced rodent models of obesity (51, 52, 78–80). Our analysis of isolated cardiac mitochondria did not indicate mitochondrial oxidative defects, uncoupling or ROS overproduction in contrast to previous studies (54, 77, 78). Unlike previous studies, our measurements of ROS synthesis were performed in real time using a mixture of substrates and a range of concentrations of ADP, but small increases in ROS may accumulate and lead to oxidative damage that may be missed by these experiments. It is difficult to explain these deviations from the literature, without comprehensive knowledge and testing of all potential environmental and methodologic variables. Of interest, recent

**Table 5.** Gene expression of hypertrophy and remodeling-related genes, metabolism-related genes, and antioxidant defense-related genes in the hearts of mice subject to dietary intervention

	HF <sub>L</sub> 10		HF <sub>L</sub> 20		HF <sub>S</sub> 10			HF <sub>S</sub> 20		
	10% Fat	60% Fat	10% Fat	60% Fat	LFLS	LFHS	HFHS	LFLS	LFHS	HFHS
<i>Hypertrophy and remodeling-related genes</i>										
<i>ANP</i>	1±0.21	1.07±0.33	1±0.09	0.53±0.14*	1±0.24	0.85±0.2	0.42±0.1	1±0.28	0.92±0.21	0.67±0.28
<i>BNP</i>	1±0.2	1.28±0.37	1±0.3	0.86±0.13	1±0.13	1.23±0.22	1.14±0.22	1±0.17	0.78±0.13	0.55±0.2
<i>Ctgf</i>	1±0.18	1.47±0.48	1±0.39	0.71±0.09	1±0.1	0.98±0.14	1.15±0.19	1±0.12	0.79±0.07	0.67±0.07
<i>Myh7</i>	1±0.3	1.12±0.14	1±0.12	1.74±0.43	1±0.14	0.97±0.15	0.84±0.22	1±0.35	1.23±0.31	0.79±0.26
<i>MMP2</i>	1±0.08	1.4±0.19	1±0.09	1.43±0.09*	1±0.09	0.97±0.06	1.28±0.08 <sup>^</sup>	1±0.04	1.19±0.05	1.29±0.04 <sup>^^</sup>
<i>MMP9</i>	1±0.15	1.53±0.24	1±0.16	1.6±0.12*	1±0.12	0.85±0.11	1.19±0.12	1±0.17	1.2±0.03	1.66±0.91
<i>Col1a1</i>	1±0.07	1.36±0.13*	1±0.06	1.59±0.11**	1±0.13	0.82±0.08	1.33±0.15	1±0.04	1.13±0.1	1.39±0.12 <sup>^</sup>
<i>Col1a2</i>	1±0.18	0.77±0.12	1±0.15	1.1±0.16	1±0.16	0.92±0.13	1.26±0.16	1±0.05	1.05±0.1	1.31±0.07
<i>Col3a1</i>	1±0.13	1.47±0.2	1±0.12	1.73±0.15	1±0.11	0.85±0.06	1.3±0.09 <sup>^</sup>	1±0.08	1.17±0.11	1.29±0.14
<i>Metabolism-related genes</i>										
<i>AcadL</i>	1±0.02	1.36±0.09**	1±0.03	1.42±0.1**	1±0.03	0.89±0.07	0.98±0.03	1±0.11	1.15±0.05	1.44±0.09 <sup>^^</sup>
<i>Acs1L</i>	1±0.05	1.15±0.06	1±0.03	1.33±0.06	1±0.05	1.02±0.03	1.39±0.08 <sup>^^</sup>	1±0.03	1.07±0.04	1.43±0.08 <sup>^^^</sup>
<i>CD36</i>	1±0.03	1.62±0.06***	1±0.05	1.55±0.08***	1±0.03	1.07±0.02	1.46±0.05 <sup>^^^</sup>	1±0.09	1.11±0.06	1.65±0.03 <sup>^^^</sup>
<i>Cpt1b</i>	1±0.03	1.41±0.06***	1±0.04	1.46±0.08***	1±0.04	1.05±0.04	1.36±0.02 <sup>^^^</sup>	1±0.04	1.13±0.05	1.22±0.04 <sup>^^</sup>
<i>Dgat1</i>	1±0.03	1.1±0.06	1±0.05	1.13±0.03	1±0.03	0.92±0.07	0.95±0.02	1±0.05	0.96±0.02	0.95±0.05
<i>Glut4</i>	1±0.03	0.82±0.05*	1±0.03	0.94±0.03	1±0.09	0.99±0.07	1.02±0.07	1±0.04	1.01±0.02	0.95±0.08
<i>Hadh</i>	1±0.03	1.37±0.1**	1±0.04	1.3±0.08**	1±0.1	0.74±0.04	0.61±0.06 <sup>^^</sup>	1±0.03	1.09±0.05	0.71±0.09 <sup>^^</sup>
<i>Pdk4</i>	1±0.36	4.08±0.5**	1±0.27	3.92±0.82**	1±0.14	1.05±0.2	2.65±0.3 <sup>^^^</sup>	1±0.22	1.24±0.09	3.59±0.54 <sup>^^^</sup>
<i>Plin5</i>	1±0.07	1.62±0.09**	1±0.1	1.92±0.17**	1±0.1	0.99±0.07	1.38±0.14 <sup>^</sup>	1±0.13	1.04±0.07	1.27±0.07
<i>Pnpla2</i>	1±0.03	1.23±0.04**	1±0.02	1.3±0.09**	1±0.14	0.84±0.09	0.78±0.13	1±0.04	0.93±0.03	0.49±0.04 <sup>^^^</sup>
<i>Scd1</i>	1±0.07	0.76±0.09	1±0.08	0.95±0.01	1±0.06	1.04±0.24	1.29±0.14	1±0.07	1.07±0.11	1.5±0.1 <sup>^^</sup>
<i>Ucp3</i>	1±0.25	1.98±0.2 *	1±0.25	1.85±0.32*	1±0.18	1.02±0.3	1.81±0.3 <sup>^</sup>	1±0.09	1.75±0.46	2±0.18 <sup>^</sup>
<i>Antioxidant defense genes</i>										
<i>Catalase</i>	1±0.04	1.54±0.09***	1±0.03	1.71±0.1****	1±0.03	1.09±0.04	1.84±0.13 <sup>^^^</sup>	1±0.04	1±0.04	1.37±0.04 <sup>^^^</sup>
<i>HO-1</i>	1±0.07	1.35±0.2	1±0.25	1.08±0.07	1±0.12	1.1±0.16	1.42±0.32	1±0.1	0.81±0.08	0.96±0.03
<i>SOD2</i>	1±0.05	1.04±0.03	1±0.03	1.17±0.05	1±0.04	1.06±0.06	1.16±0.07	1±0.03	1.02±0.03	1.08±0.03

Values are means ± SE. Composition of the diets are described in Supplemental Table S1. HF<sub>L</sub> 10 and HF<sub>L</sub> 20 refer to mice that were 10 wk of age or 20 wk of age, respectively, at the time of initiation with lard-based diets. HF<sub>S</sub> 10 and HF<sub>S</sub> 20 refer to mice that were 10 wk of age or 20 wk of age, respectively, at the time of initiation with saturated fat-based diets. HFHS, high-fat high-sucrose; LFHS, low-fat high-sucrose; LFLS, low-fat low-sucrose; LS, low sucrose. Statistical testing was performed within each age group. Data were analyzed by *t* test for within age group comparisons in mice fed lard-based diet and by one-way ANOVA followed by post hoc analysis using Tukey's test in mice fed saturated fat-rich diet. \**P* < 0.05, \*\**P* < 0.01, \*\*\**P* < 0.001, and \*\*\*\**P* < 0.0001, statistical significance in lard-based diet groups; and <sup>^</sup>*P* < 0.05, <sup>^^</sup>*P* < 0.01, <sup>^^^</sup>*P* < 0.001, and <sup>^^^</sup>*P* < 0.0001, statistical significance in saturated fat-based diet groups (*n* > 6 animals/group).

studies suggest that phenotypic differences in metabolism in mice of identical genotypes and genetic background but housed in different animal facilities can be explained by differences in the gut microbiome. (81).

The background strain of mice and environmental factors are important considerations (82–84) for studies of metabolism given the fact that baseline differences indeed exist among the various strains in parameters such as liver enzymes and plasma lipid profiles (85). Such differences could contribute to differences in insulin release and metabolic profiles of mice fed fat-enriched diet, where various substrains were used (86). However, in the multiple cohorts used for the data presented within our study, we consistently observed insulin resistance and glucose intolerance, independent of the background strain. Therefore, the lack of a phenotype consistent with cardiac dysfunction in the face of persistent metabolic perturbations suggests that cardiac dysfunction in the face of dysmetabolic state may not manifest in mice consistently unless fat feeding is performed for substantially longer durations (>16 mo) and even then might only manifest after an acute inotropic stress (87) or when an additional pathological state such as overt hypertension or vascular dysfunction is superimposed, as reported recently (88). Moreover, evidence of mitochondrial dysfunction and fibrosis was evident in another study only after >18 mo of

high-fat feeding, although systolic dysfunction did not develop (89). It is important to note that the custom-ordered diets used in our studies were matched for sucrose content, whereas the only variable between the control diets and the experimental diets was the percent calories derived from fat. This enabled us to negate the possible confounding effects of variable sucrose content between commonly used control and high-fat diets and allowed us to thoroughly investigate the effects of dietary fat overload on whole body metabolism and on cardiac function.

It is also possible that the lack of cardiac functional phenotype in the various high-fat-fed groups may indicate robust compensatory responses, which may have contributed to the preserved cardiac function. Although we failed to uncover a cardiac functional phenotype using the techniques at our disposal, we reproducibly observed cardiac hypertrophy in high-fat-fed mice with the hypertrophic phenotype being more pronounced in younger mice fed a high-fat diet than older mice. However, when we probed for markers of pathological cardiac hypertrophy, we did not observe significant increases in natriuretic peptides—ANP and BNP that are induced by increased wall stress, nor did we note elevations in Myh7—the isoform that is induced under pathological conditions. We also investigated whether the high-fat-fed mice exhibited increased fibrosis in their hearts and found



no significant differences between control and high-fat groups. Modest, but significant increases in expression levels of collagen transcripts were found in hearts of high-fat-fed groups but these increases were not associated with collagen accumulation or cardiac fibrosis.

### Limitations

Our findings suggest that high-fat feeding in C57BL/6J mice may not represent a reproducible model to study mechanisms of diabetic cardiomyopathy, defined as ventricular dysfunction and fibrosis. The use of a single strain of mice in this study however does not inform whether other strains may be sensitive to cardiac dysfunction induced by metabolic stress. We used 2-D echocardiography and LV catheterization to measure cardiac function and both these techniques measure cardiac function in a load-dependent manner. Use of a gold-standard technique such as PV-loops could identify subtle cardiac functional deficits that we were unable to uncover with conventional techniques. We assessed mitochondrial function using the whole mitochondrial fraction. Specific isolation procedures may allow for assessment of whether there may be differences in sensitivity of the subpopulations (subsarcolemmal and interfibrillar) to dietary fat overload-induced metabolic stress.

### Summary

High-fat diet feeding regardless of saturation content of the fat might not be sufficient to induce cardiac dysfunction in C57BL/6J mice. In this study, we found that mitochondrial function is not impaired by fat feeding. Lipid accumulation following high-fat feeding is modest, possibly due to an increased fatty acid oxidation and utilization in the myocardium of fat-fed mice. These results highlight resilience of the mouse heart to cardiac dysfunction following metabolic stress, in the absence of additional variables that remain to be definitively identified.

### SUPPLEMENTAL DATA

Supplemental Fig. S1: <https://doi.org/10.6084/m9.figshare.15050733>

Supplemental Fig. S2: <https://doi.org/10.6084/m9.figshare.15050730>

Supplemental Fig. S3: <https://doi.org/10.6084/m9.figshare.15050724>

Supplemental Table S1: <https://doi.org/10.6084/m9.figshare.15050718>

Supplemental Table S2: <https://doi.org/10.6084/m9.figshare.15050721>

Supplemental Table S3: <https://doi.org/10.6084/m9.figshare.15050727>.

### ACKNOWLEDGMENTS

We thank Dr. Yang K. Xiang (UC Davis, CA) for providing the GRK2-floxed mice used in this study. We also thank Brett Wagner, Jamie Soto, and Dr. Chantal Allamargot for their technical assistance. The data presented herein were obtained at the Metabolic Phenotyping Core, Electron Spin Resonance Facility, and the Central Microscopy Research Facility, which are core research facilities within the Carver College of Medicine at the University of Iowa.

### GRANTS

This research was supported by National Institutes of Health (NIH) Grants R01HL12413 and R01HL127764, American Heart Association Grant 20SFRN35120123 (to E. D. Abel), NIH Grants S10OD019941 and R01HL142935 (to R. M. Weiss), and Veterans Affairs Merit Review Award IO1 BXOO4468 (to B. T. O'Neill.). The ESR Facility at The University of Iowa is supported in part by NIH Grants P01 CA217797 and P30 CA086862.

### DISCLOSURES

No conflicts of interest, financial or otherwise, are declared by the authors.

### AUTHOR CONTRIBUTIONS

S.M.T., B.T.O., and E.D.A. conceived and designed research; S.M.T., E.T.W., G.V.C., G.B., J.C., W.K., K.Z., and A.B. performed experiments; S.M.T., E.T.W., G.V.C., G.B., J.C., K.Z., A.B., R.M.W., and E.D.A. analyzed data; S.M.T., G.B., B.T.O., R.M.W., and E.D.A. interpreted results of experiments; S.M.T. prepared figures; S.M.T. and E.D.A. drafted manuscript; S.M.T., B.T.O., R.M.W., and E.D.A. edited and revised manuscript; S.M.T., E.T.W., G.V.C., G.B., J.C., W.K., K.Z., A.B., B.T.O., R.M.W., and E.D.A. approved final version of manuscript.

### REFERENCES

1. **Murphy SL, Xu J, Kochanek KD, Arias E.** Mortality in the United States, 2017. NCHS data brief, no 328. Hyattsville, MD: National Center for Health Statistics; 2018.
2. **Kannel WB, Hjortland M, Castelli WP.** Role of diabetes in congestive heart failure: the Framingham study. *Am J Cardiol* 34: 29–34, 1974. doi:10.1016/0002-9149(74)90089-7.
3. **Kannel WB, McGee DL.** Diabetes and cardiovascular disease. The Framingham study. *JAMA* 241: 2035–2038, 1979. doi:10.1001/jama.241.19.2035.
4. **Galderisi M, Anderson KM, Wilson PW, Levy D.** Echocardiographic evidence for the existence of a distinct diabetic cardiomyopathy (the Framingham Heart Study). *Am J Cardiol* 68: 85–89, 1991. doi:10.1016/0002-9149(91)90716-X.
5. **Kenchaiah S, Evans JC, Levy D, Wilson PW, Benjamin EJ, Larson MG, Kannel WB, Vasan RS.** Obesity and the risk of heart failure. *N Engl J Med* 347: 305–313, 2002. doi:10.1056/NEJMoa020245.
6. **Lauer MS, Anderson KM, Kannel WB, Levy D.** The impact of obesity on left ventricular mass and geometry. The Framingham Heart Study. *JAMA* 266: 231–236, 1991. doi:10.1001/jama.1991.03470020057032.
7. **DebBurman SK, Ptasinski J, Benovic JL, Hosey MM.** G protein-coupled receptor kinase GRK2 is a phospholipid-dependent enzyme that can be conditionally activated by G protein beta-gamma subunits. *J Biol Chem* 271: 22552–22562, 1996. doi:10.1074/jbc.271.37.22552.
8. **Evron T, Daigle TL, Caron MG.** GRK2: multiple roles beyond G protein-coupled receptor desensitization. *Trends Pharmacol Sci* 33: 154–164, 2012. doi:10.1016/j.tips.2011.12.003.
9. **Huang ZM, Gao E, Chuprun JK, Koch WJ.** GRK2 in the heart: a GPCR kinase and beyond. *Antioxid Redox Signal* 21: 2032–2043, 2014. doi:10.1089/ars.2014.5876.
10. **Chen M, Sato PY, Chuprun JK, Peroutka RJ, Otis NJ, Ibetti J, Pan S, Sheu SS, Gao E, Koch WJ.** Prodeath signaling of G protein-coupled receptor kinase 2 in cardiac myocytes after ischemic stress occurs via extracellular signal-regulated kinase-dependent heat shock protein 90-mediated mitochondrial targeting. *Circ Res* 112: 1121–1134, 2013. doi:10.1161/CIRCRESAHA.112.300754.
11. **Fan Q, Chen M, Zuo L, Shang X, Huang MZ, Ciccarelli M, Raake P, Brinks H, Chuprun KJ, Dorn GW 2nd, Koch WJ, Gao E.** Myocardial ablation of G protein-coupled receptor kinase 2 (GRK2) decreases ischemia/reperfusion injury through an anti-intrinsic apoptotic pathway. *PLoS One* 8: e66234, 2013. doi:10.1371/journal.pone.0066234.

12. Iaccarino G, Barbato E, Cipolletta E, De Amicis V, Margulies KB, Leosco D, Trimarco B, Koch WJ. Elevated myocardial and lymphocyte GRK2 expression and activity in human heart failure. *Eur Heart J* 26: 1752–1758, 2005. doi:10.1093/eurheartj/ehi429.
13. Raake PW, Vinge LE, Gao E, Boucher M, Rengo G, Chen X, DeGeorge BR Jr, Matkovich S, Houser SR, Most P, Eckhart AD, Dorn GW 2nd, Koch WJ. G protein-coupled receptor kinase 2 ablation in cardiac myocytes before or after myocardial infarction prevents heart failure. *Circ Res* 103: 413–422, 2008. doi:10.1161/CIRCRESAHA.107.168336.
14. Raake PW, Zhang X, Vinge LE, Brinks H, Gao E, Jaleel N, Li Y, Tang M, Most P, Dorn GW 2nd, Houser SR, Katus HA, Chen X, Koch WJ. Cardiac G-protein-coupled receptor kinase 2 ablation induces a novel Ca<sup>2+</sup> handling phenotype resistant to adverse alterations and remodeling after myocardial infarction. *Circulation* 125: 2108–2118, 2012. doi:10.1161/CIRCULATIONAHA.111.044255.
15. Sato PY, Chuprun JK, Grisanti LA, Woodall MC, Brown BR, Roy R, Traynham CJ, Ibbett J, Lucchese AM, Yuan A, Drosatos K, Tilley DG, Gao E, Koch WJ. Restricting mitochondrial GRK2 post-ischemia confers cardioprotection by reducing myocyte death and maintaining glucose oxidation. *Sci Signal* 11: eaau0144, 2018. doi:10.1126/scisignal.aau0144.
16. Schlegel P, Reinkober J, Meinhardt E, Tscheschner H, Gao E, Schumacher SM, Yuan A, Backs J, Most P, Wieland T, Koch WJ, Katus HA, Raake PW. G protein-coupled receptor kinase 2 promotes cardiac hypertrophy. *PLoS One* 12: e0182110, 2017. doi:10.1371/journal.pone.0182110.
17. Lucas E, Vila-Bedmar R, Arcones AC, Cruces-Sande M, Cachafeiro V, Mayor F Jr, Murga C. Obesity-induced cardiac lipid accumulation in adult mice is modulated by G protein-coupled receptor kinase 2 levels. *Cardiovasc Diabetol* 15: 155, 2016. doi:10.1186/s12933-016-0474-6.
18. Wang Q, Liu Y, Fu Q, Xu B, Zhang Y, Kim S, Tan R, Barbagallo F, West T, Anderson E, Wei W, Abel ED, Xiang YK. Inhibiting insulin-mediated  $\beta$ 2-adrenergic receptor activation prevents diabetes-associated cardiac dysfunction. *Circulation* 135: 73–88, 2017. doi:10.1161/CIRCULATIONAHA.116.022281.
19. Abd Alla J, Graemer M, Fu X, Quittner U. Inhibition of G-protein-coupled receptor kinase 2 prevents the dysfunctional cardiac substrate metabolism in fatty acid synthase transgenic mice. *J Biol Chem* 291: 2583–2600, 2016. doi:10.1074/jbc.M115.702688.
20. Pflieger J, Gross P, Johnson J, Carter RL, Gao E, Tilley DG, Houser SR, Koch WJ. G protein-coupled receptor kinase 2 contributes to impaired fatty acid metabolism in the failing heart. *J Mol Cell Cardiol* 123: 108–117, 2018. doi:10.1016/j.jmcc.2018.08.025.
21. Sato PY, Chuprun JK, Ibbett J, Cannavo A, Drosatos K, Elrod JW, Koch WJ. GRK2 compromises cardiomyocyte mitochondrial function by diminishing fatty acid-mediated oxygen consumption and increasing superoxide levels. *J Mol Cell Cardiol* 89(Pt B): 360–364, 2015. doi:10.1016/j.jmcc.2015.10.002.
22. Belke DD, Larsen TS, Gibbs EM, Severson DL. Altered metabolism causes cardiac dysfunction in perfused hearts from diabetic (db/db) mice. *Am J Physiol Endocrinol Metab* 279: E1104–E1113, 2000. doi:10.1152/ajpendo.2000.279.5.E1104.
23. Semeniuk LM, Kryski AJ, Severson DL. Echocardiographic assessment of cardiac function in diabetic db/db and transgenic db/db-hGLUT4 mice. *Am J Physiol Heart Circ Physiol* 283: H976–H982, 2002. doi:10.1152/ajpheart.00088.2002.
24. Buchanan J, Mazumder PK, Hu P, Chakrabarti G, Roberts MW, Yun UJ, Cooksey RC, Litwin SE, Abel ED. Reduced cardiac efficiency and altered substrate metabolism precedes the onset of hyperglycemia and contractile dysfunction in two mouse models of insulin resistance and obesity. *Endocrinology* 146: 5341–5349, 2005. doi:10.1210/en.2005-0938.
25. Christoffersen C, Bollano E, Lindegaard ML, Bartels ED, Goetze JP, Andersen CB, Nielsen LB. Cardiac lipid accumulation associated with diastolic dysfunction in obese mice. *Endocrinology* 144: 3483–3490, 2003. doi:10.1210/en.2003-0242.
26. Dong F, Zhang X, Yang X, Esberg LB, Yang H, Zhang Z, Culver B, Ren J. Impaired cardiac contractile function in ventricular myocytes from leptin-deficient ob/ob obese mice. *J Endocrinol* 188: 25–36, 2006. doi:10.1677/joe.1.06241.
27. Mazumder PK, O'Neill BT, Roberts MW, Buchanan J, Yun UJ, Cooksey RC, Boudina S, Abel ED. Impaired cardiac efficiency and increased fatty acid oxidation in insulin-resistant ob/ob mouse hearts. *Diabetes* 53: 2366–2374, 2004. doi:10.2337/diabetes.53.9.2366.
28. Chiu HC, Kovacs A, Ford DA, Hsu FF, Garcia R, Herrero P, Saffitz JE, Schaffer JE. A novel mouse model of lipotoxic cardiomyopathy. *J Clin Invest* 107: 813–822, 2001. doi:10.1172/JCI10947.
29. Liu L, Shi X, Bharadwaj KG, Ikeda S, Yamashita H, Yagyu H, Schaffer JE, Yu YH, Goldberg IJ. DGAT1 expression increases heart triglyceride content but ameliorates lipotoxicity. *J Biol Chem* 284: 36312–36323, 2009. doi:10.1074/jbc.M109.049817.
30. Park SY, Cho YR, Kim HJ, Higashimori T, Danton C, Lee MK, Dey A, Rothermel B, Kim YB, Kalinowski A, Russell KS, Kim JK. Unraveling the temporal pattern of diet-induced insulin resistance in individual organs and cardiac dysfunction in C57BL/6 mice. *Diabetes* 54: 3530–3540, 2005. doi:10.2337/diabetes.54.12.3530.
31. Battiprolu PK, Hojaye B, Jiang N, Wang ZV, Luo X, Iglewski M, Shelton JM, Gerard RD, Rothermel BA, Gillette TG, Lavandero S, Hill JA. Metabolic stress-induced activation of FoxO1 triggers diabetic cardiomyopathy in mice. *J Clin Invest* 122: 1109–1118, 2012. doi:10.1172/JCI60329.
32. Brainard RE, Watson LJ, DeMartino AM, Brittan KR, Readnower RD, Boakye AA, Zhang D, Hoetker JD, Bhatnagar A, Baba SP, Jones SP. High fat feeding in mice is insufficient to induce cardiac dysfunction and does not exacerbate heart failure. *PLoS One* 8: e83174, 2013. [Erratum in *PLoS One* 9: e113944, 2019]. doi:10.1371/journal.pone.0083174.
33. Gupte AA, Minze LJ, Reyes M, Ren Y, Wang X, Brunner G, Ghosh M, Cordero-Reyes AM, Ding K, Pratico D, Morrisett J, Shi ZZ, Hamilton DJ, Lyon CJ, Hsueh WA. High-fat feeding-induced hyperinsulinemia increases cardiac glucose uptake and mitochondrial function despite peripheral insulin resistance. *Endocrinology* 154: 2650–2662, 2013. doi:10.1210/en.2012-2272.
34. Matkovich SJ, Diwan A, Klanke JL, Hammer DJ, Marreez Y, Odley AM, Brunsell EW, Koch WJ, Schwartz RJ, Dorn GW 2nd. Cardiac-specific ablation of G-protein receptor kinase 2 redefines its roles in heart development and  $\beta$ -adrenergic signaling. *Circ Res* 99: 996–1003, 2006. doi:10.1161/01.RES.0000247932.71270.2c.
35. Makrecka-Kuka M, Krumschnabel G, Nagra E. High-resolution respirometry for simultaneous measurement of oxygen and hydrogen peroxide fluxes in permeabilized cells, tissue homogenate and isolated mitochondria. *Biomolecules* 5: 1319–1338, 2015. doi:10.3390/biom5031319.
36. Penniman CM, Suarez Beltran PA, Bhardwaj G, Junck TL, Jena J, Poro K, Hirshman MF, Goodyear LJ, O'Neill BT. Loss of FoxOs in muscle reveals sex-based differences in insulin sensitivity but mitigates diet-induced obesity. *Mol Metab* 30: 203–220, 2019. doi:10.1016/j.molmet.2019.10.001.
37. Lark DS, Torres MJ, Lin CT, Ryan TE, Anderson EJ, Neuffer PD. Direct real-time quantification of mitochondrial oxidative phosphorylation efficiency in permeabilized skeletal muscle myofibers. *Am J Physiol Cell Physiol* 311: C239–C245, 2016. doi:10.1152/ajpcell.00124.2016.
38. Barnabei MS, Palpant NJ, Metzger JM. Influence of genetic background on ex vivo and in vivo cardiac function in several commonly used inbred mouse strains. *Physiol Genomics* 42a: 103–113, 2010. doi:10.1152/physiolgenomics.00071.2010.
39. Barrick CJ, Rojas M, Schoonhoven R, Smyth SS, Threadgill DW. Cardiac response to pressure overload in 129S1/SvImJ and C57BL/6J mice: temporal- and background-dependent development of concentric left ventricular hypertrophy. *Am J Physiol Heart Circ Physiol* 292: H2119–H2130, 2007. doi:10.1152/ajpheart.00816.2006.
40. Garcia-Menendez L, Karamanlidis G, Kolwicz S, Tian R. Substrain specific response to cardiac pressure overload in C57BL/6 mice. *Am J Physiol Heart Circ Physiol* 305: H397–H402, 2013. doi:10.1152/ajpheart.00088.2013.
41. Jelinek M, Wallach C, Ehmke H, Schwoerer AP. Genetic background dominates the susceptibility to ventricular arrhythmias in a murine model of  $\beta$ -adrenergic stimulation. *Sci Rep* 8: 2312, 2018. doi:10.1038/s41598-018-20792-5.
42. Shah AP, Siedlecka U, Gandhi A, Navaratnarajah M, Al-Saud SA, Yacoub MH, Terracciano CM. Genetic background affects function and intracellular calcium regulation of mouse hearts. *Cardiovasc Res* 87: 683–693, 2010. doi:10.1093/cvr/cvq111.

43. Toye AA, Lippiat JD, Proks P, Shimomura K, Bentley L, Hugill A, Mijat V, Goldsworthy M, Moir L, Haynes A, Quartermann J, Freeman HC, Ashcroft FM, Cox RD. A genetic and physiological study of impaired glucose homeostasis control in C57BL/6J mice. *Diabetologia* 48: 675–686, 2005. doi:10.1007/s00125-005-1680-z.
44. Scarborough P, Rayner M, van Dis I, Norum K. Meta-analysis of effect of saturated fat intake on cardiovascular disease: overadjustment obscures true associations. *Am J Clin Nutr* 92: 458–459, 2010. doi:10.3945/ajcn.2010.29504.
45. Siri-Tarino PW, Sun Q, Hu FB, Krauss RM. Meta-analysis of prospective cohort studies evaluating the association of saturated fat with cardiovascular disease. *Am J Clin Nutr* 91: 535–546, 2010. doi:10.3945/ajcn.2009.27725.
46. de Souza RJ, Mente A, Maroleanu A, Cozma AI, Ha V, Kishibe T, Uleryk E, Budylowski P, Schünemann H, Beyene J, Anand SS. Intake of saturated and trans unsaturated fatty acids and risk of all cause mortality, cardiovascular disease, and type 2 diabetes: systematic review and meta-analysis of observational studies. *BMJ* 351: h3978, 2015. doi:10.1136/bmj.h3978.
47. Listenberger LL, Han X, Lewis SE, Cases S, Farese RV Jr, Ory DS, Schaffer JE. Triglyceride accumulation protects against fatty acid-induced lipotoxicity. *Proc Natl Acad Sci USA* 100: 3077–3082, 2003. doi:10.1073/pnas.0630588100.
48. Miller TA, LeBrasseur NK, Cote GM, Trucillo MP, Pimentel DR, Ido Y, Ruderman NB, Sawyer DB. Oleate prevents palmitate-induced cytotoxic stress in cardiac myocytes. *Biochem Biophys Res Commun* 336: 309–315, 2005. doi:10.1016/j.bbrc.2005.08.088.
49. Bugger H, Abel ED. Molecular mechanisms of diabetic cardiomyopathy. *Diabetologia* 57: 660–671, 2014. doi:10.1007/s00125-014-3171-6.
50. Wende AR, Abel ED. Lipotoxicity in the heart. *Biochim Biophys Acta* 1801: 311–319, 2010. doi:10.1016/j.bbalip.2009.09.023.
51. Boudina S, Han YH, Pei S, Tidwell TJ, Henrie B, Tuinei J, Olsen C, Sena S, Abel ED. UCP3 regulates cardiac efficiency and mitochondrial coupling in high fat-fed mice but not in leptin-deficient mice. *Diabetes* 61: 3260–3269, 2012. doi:10.2337/db12-0063.
52. Chen D, Li X, Zhang L, Zhu M, Gao L. A high-fat diet impairs mitochondrial biogenesis, mitochondrial dynamics, and the respiratory chain complex in rat myocardial tissues. *J Cell Biochem* 119: 9602, 2018. doi:10.1002/jcb.27068.
53. Marciniak C, Marechal X, Montaigne D, Neviere R, Lancel S. Cardiac contractile function and mitochondrial respiration in diabetes-related mouse models. *Cardiovasc Diabetol* 13: 118, 2014. doi:10.1186/s12933-014-0118-7.
54. Sverdlow AL, Elezaby A, Behring JB, Bachschmid MM, Luptak I, Tu VH, Siwik DA, Miller EJ, Liesa M, Shirihai OS, Pimentel DR, Cohen RA, Colucci WS. High fat, high sucrose diet causes cardiac mitochondrial dysfunction due in part to oxidative post-translational modification of mitochondrial complex II. *J Mol Cell Cardiol* 78: 165–173, 2015. doi:10.1016/j.yjmcc.2014.07.018.
55. Cole MA, Murray AJ, Cochlin LE, Heather LC, McAleese S, Knight NS, Sutton E, Jamil AA, Parassol N, Clarke K. A high fat diet increases mitochondrial fatty acid oxidation and uncoupling to decrease efficiency in rat heart. *Basic Res Cardiol* 106: 447–457, 2011. doi:10.1007/s00395-011-0156-1.
56. Fang ZY, Prins JB, Marwick TH. Diabetic cardiomyopathy: evidence, mechanisms, and therapeutic implications. *Endocr Rev* 25: 543–567, 2004. doi:10.1210/er.2003-0012.
57. Boudina S, Abel ED. Diabetic cardiomyopathy, causes and effects. *Rev Endocr Metab Disord* 11: 31–39, 2010. doi:10.1007/s11554-010-9131-7.
58. Lucas E, Jurado-Pueyo M, Fortuño MA, Fernández-Veledo S, Vila-Bedmar R, Jiménez-Borreguero LJ, Lazcano JJ, Gao E, Gómez-Ambrosi J, Frühbeck G, Koch WJ, Díez J, Mayor F Jr, Murga C. Downregulation of G protein-coupled receptor kinase 2 levels enhances cardiac insulin sensitivity and switches on cardioprotective gene expression patterns. *Biochim Biophys Acta* 1842: 2448–2456, 2014. doi:10.1016/j.bbdis.2014.09.004.
59. Vila-Bedmar R, Cruces-Sande M, Lucas E, Willemen HL, Heijnen CJ, Kavelaars A, Mayor F Jr, Murga C. Reversal of diet-induced obesity and insulin resistance by inducible genetic ablation of GRK2. *Sci Signal* 8: ra73, 2015. doi:10.1126/scisignal.aaa4374.
60. Ouwers DM, Boer C, Fodor M, de Galan P, Heine RJ, Maassen JA, Diamant M. Cardiac dysfunction induced by high-fat diet is associated with altered myocardial insulin signalling in rats. *Diabetologia* 48: 1229–1237, 2005. doi:10.1007/s00125-005-1755-x.
61. Ouwers DM, Diamant M, Fodor M, Habets DDJ, Pelsers MMAL, El Hasnaoui M, Dang ZC, van den Brom CE, Vlasblom R, Rietdijk A, Boer C, Coort SLM, Glatz JFC, Luiken JJFP. Cardiac contractile dysfunction in insulin-resistant rats fed a high-fat diet is associated with elevated CD36-mediated fatty acid uptake and esterification. *Diabetologia* 50: 1938–1948, 2007. doi:10.1007/s00125-007-0735-8.
62. Collins S, Martin TL, Surwit RS, Robidoux J. Genetic vulnerability to diet-induced obesity in the C57BL/6J mouse: physiological and molecular characteristics. *Physiol Behav* 81: 243–248, 2004. doi:10.1016/j.physbeh.2004.02.006.
63. Cao L, Qin X, Peterson MR, Haller SE, Wilson KA, Hu N, Lin X, Nair S, Ren J, He G. CARD9 knockout ameliorates myocardial dysfunction associated with high fat diet-induced obesity. *J Mol Cell Cardiol* 92: 185–195, 2016. doi:10.1016/j.yjmcc.2016.02.014.
64. Ceylan-Isik AF, Kandadi MR, Xu X, Hua Y, Chicco AJ, Ren J, Nair S. Apelin administration ameliorates high fat diet-induced cardiac hypertrophy and contractile dysfunction. *J Mol Cell Cardiol* 63: 4–13, 2013. doi:10.1016/j.yjmcc.2013.07.002.
65. Fang CX, Dong F, Thomas PD, Ma H, He L, Ren J. Hypertrophic cardiomyopathy in high-fat diet-induced obesity: role of suppression of forkhead transcription factor and atrophy gene transcription. *Am J Physiol Heart Circ Physiol* 295: H1206–H1215, 2008. doi:10.1152/ajpheart.00319.2008.
66. Hu N, Zhang Y. TLR4 knockout attenuated high fat diet-induced cardiac dysfunction via NF- $\kappa$ B/JNK-dependent activation of autophagy. *Biochim Biophys Acta Mol Basis Dis* 1863: 2001–2011, 2017. doi:10.1016/j.bbdis.2017.01.010.
67. Hua Y, Zhang Y, Dolence J, Shi GP, Ren J, Nair S. Cathepsin K knockout mitigates high-fat diet-induced cardiac hypertrophy and contractile dysfunction. *Diabetes* 62: 498–509, 2013. doi:10.2337/db12-0350.
68. Popp RL, Rubenson DS, Tucker CR, French JW. Echocardiography: M-mode and two-dimensional methods. *Ann Intern Med* 93: 844–856, 1980. doi:10.7326/0003-4819-93-6-844.
69. Chess DJ, Lei B, Hoit BD, Azimzadeh AM, Stanley WC. Effects of a high saturated fat diet on cardiac hypertrophy and dysfunction in response to pressure overload. *J Card Fail* 14: 82–88, 2008. doi:10.1016/j.cardfail.2007.09.004.
70. Okere IC, Chandler MP, McElfresh TA, Rennison JH, Sharov V, Sabbah HN, Tserng KY, Hoit BD, Ernberger P, Young ME, Stanley WC. Differential effects of saturated and unsaturated fatty acid diets on cardiomyocyte apoptosis, adipose distribution, and serum leptin. *Am J Physiol Heart Circ Physiol* 291: H38–H44, 2006. doi:10.1152/ajpheart.01295.2005.
71. Okere IC, Chess DJ, McElfresh TA, Johnson J, Rennison J, Ernberger P, Hoit BD, Chandler MP, Stanley WC. High-fat diet prevents cardiac hypertrophy and improves contractile function in the hypertensive Dahl salt-sensitive rat. *Clin Exp Pharmacol Physiol* 32: 825–831, 2005. doi:10.1111/j.1440-1681.2005.04272.x.
72. Berthiaume JM, Bray MS, McElfresh TA, Chen X, Azam S, Young ME, Hoit BD, Chandler MP. The myocardial contractile response to physiological stress improves with high saturated fat feeding in heart failure. *Am J Physiol Heart Circ Physiol* 299: H410–H421, 2010. doi:10.1152/ajpheart.00270.2010.
73. Berthiaume JM, Young ME, Chen X, McElfresh TA, Yu X, Chandler MP. Normalizing the metabolic phenotype after myocardial infarction: impact of subchronic high fat feeding. *J Mol Cell Cardiol* 53: 125–133, 2012. doi:10.1016/j.yjmcc.2012.04.005.
74. Christopher BA, Huang HM, Berthiaume JM, McElfresh TA, Chen X, Croniger CM, Muzic RF Jr, Chandler MP. Myocardial insulin resistance induced by high fat feeding in heart failure is associated with preserved contractile function. *Am J Physiol Heart Circ Physiol* 299: H1917–H1927, 2010. doi:10.1152/ajpheart.00687.2010.
75. Morgan EE, Rennison JH, Young ME, McElfresh TA, Kung TA, Tserng KY, Hoit BD, Stanley WC, Chandler MP. Effects of chronic activation of peroxisome proliferator-activated receptor- $\alpha$  or high-fat feeding in a rat infarct model of heart failure. *Am J Physiol Heart Circ Physiol* 290: H1899–H1904, 2006. doi:10.1152/ajpheart.01014.2005.
76. Rennison JH, McElfresh TA, Chen X, Anand VR, Hoit BD, Hoppel CL, Chandler MP. Prolonged exposure to high dietary lipids is not associated with lipotoxicity in heart failure. *J Mol Cell Cardiol* 46: 883–890, 2009. doi:10.1016/j.yjmcc.2009.02.019.



77. Abdurrachim D, Ciapaite J, Wessels B, Nabben M, Luiken J, Nicolay K, Prompers JJ. Cardiac diastolic dysfunction in high-fat diet fed mice is associated with lipotoxicity without impairment of cardiac energetics in vivo. *Biochim Biophys Acta* 1842: 1525–1537, 2014. doi:10.1016/j.bbalip.2014.07.016.
78. Sverdlow AL, Elezaby A, Qin F, Behring JB, Luptak I, Calamaras TD, Siwik DA, Miller EJ, Liesa M, Shiriha OS, Pimentel DR, Cohen RA, Bachschmid MM, Colucci WS. Mitochondrial reactive oxygen species mediate cardiac structural, functional, and mitochondrial consequences of diet-induced metabolic heart disease. *J Am Heart Assoc* 5: e002555, 2016. doi:10.1161/JAHA.115.002555.
79. Anderson EJ, Kypson AP, Rodriguez E, Anderson CA, Lehr EJ, Neuffer PD. Substrate-specific derangements in mitochondrial metabolism and redox balance in the atrium of the type 2 diabetic human heart. *J Am Coll Cardiol* 54: 1891–1898, 2009. doi:10.1016/j.jacc.2009.07.031.
80. Boudina S, Sena S, Theobald H, Sheng X, Wright JJ, Hu X, Aziz S, Johnson JI, Bugger H, Zaha VG, Abel ED. Mitochondrial energetics in the heart in obesity-related diabetes direct evidence for increased uncoupled respiration and activation of uncoupling proteins. *Diabetes* 56: 2457–2466, 2007. doi:10.2337/db07-0481.
81. Ussar S, Griffin NW, Bezy O, Fujisaka S, Vienberg S, Softic S, Deng L, Bry L, Gordon JI, Kahn CR. Interactions between gut microbiota, host genetics and diet modulate the predisposition to obesity and metabolic syndrome. *Cell Metab* 22: 516–530, 2015. [Erratum in *Cell Metab* 23: 564–566, 2016]. doi:10.1016/j.cmet.2015.07.007.
82. Fontaine DA, Davis DB. Attention to background strain is essential for metabolic research: C57BL/6 and the international knockout mouse consortium. *Diabetes* 65: 25–33, 2016. doi:10.2337/db15-0982.
83. Rendina-Ruedy E, Hembree KD, Sasaki A, Davis MR, Lightfoot SA, Clarke SL, Lucas EA, Smith BJ. A comparative study of the metabolic and skeletal response of C57BL/6J and C57BL/6N mice in a diet-induced model of type 2 diabetes. *J Nutr Metab* 2015: 758080, 2015. doi:10.1155/2015/758080.
84. Fisher-Wellman KH, Ryan TE, Smith CD, Gilliam LA, Lin CT, Reese LR, Torres MJ, Neuffer PD. A direct comparison of metabolic responses to high-fat diet in C57BL/6J and C57BL/6NJ mice. *Diabetes* 65: 3249–3261, 2016. doi:10.2337/db16-0291.
85. Otto GP, Rathkolb B, Oestereich MA, Lenggner CJ, Moerth C, Micklich K, Fuchs H, Gailus-Durner V, Wolf E, Hrabeo de Angelis M. Clinical chemistry reference intervals for C57BL/6J, C57BL/6N, and C3HeB/FeJ mice (*Mus musculus*). *J Am Assoc Lab Anim Sci* 55: 375–386, 2016.
86. Hull RL, Willard JR, Struck MD, Barrow BM, Brar GS, Andrikopoulos S, Zraika S. High fat feeding unmasks variable insulin responses in male C57BL/6 mouse substrains. *J Endocrinol* 233: 53–64, 2017. doi:10.1530/JOE-16-0377.
87. Calligaris SD, Lecanda M, Solis F, Ezquer M, Gutiérrez J, Brandan E, Leiva A, Sobrevia L, Conget P. Mice long-term high-fat diet feeding recapitulates human cardiovascular alterations: an animal model to study the early phases of diabetic cardiomyopathy. *PLoS One* 8: e60931, 2013. doi:10.1371/journal.pone.0060931.
88. Schiattarella GG, Altamirano F, Tong D, French KM, Villalobos E, Kim SY, Luo X, Jiang N, May HI, Wang ZV, Hill TM, Mammen PPA, Huang J, Lee DI, Hahn VS, Sharma K, Kass DA, Lavandro S, Gillette TG, Hill JA. Nitrosative stress drives heart failure with preserved ejection fraction. *Nature* 568: 351–356, 2019. doi:10.1038/s41586-019-1100-z.
89. Aurich AC, Niemann B, Pan R, Gruenler S, Issa H, Silber RE, Rohrbach S. Age-dependent effects of high fat-diet on murine left ventricles: role of palmitate. *Basic Res Cardiol* 108: 369, 2013. doi:10.1007/s00395-013-0369-6.